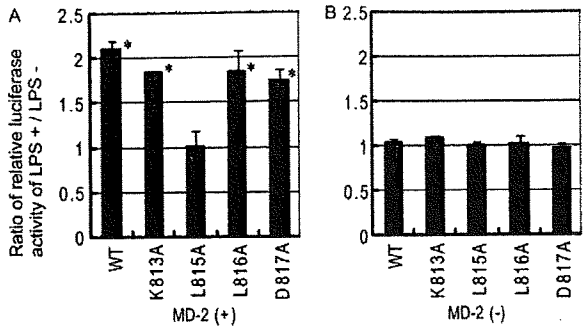


FIGURE 6. **Leucine at position 815 of TLR4 is pivotal for LPS responsiveness as measured by NF-κB luciferase assay.** *A*, HEK293T cells were transfected with single amino acid replacement mutants of the human TLR4-EGFP fusion protein plasmid, human MD-2 plasmid, and luciferase reporter and control plasmids. After 36 h, cells were stimulated with LPS (10 ng/ml) for 7 h, and luciferase reporter gene activity was measured. *B*, instead of MD-2, an empty vector was cotransfected with TLR4-EGFP plasmid and reporter assay vectors. LPS stimulation was done as in *A*. All results were expressed in the ratio of relative luciferase activity with LPS stimulation to that without the stimulation as in Fig. 2. The data were from three independent experiments. *Small bars* indicate 95% confidence intervals of the mean (*p* values for * are: TLR4 (WT)-EGFP/MD-2 (+), $p = 0.002$; TLR4 (K813A)-EGFP/MD-2 (+), $p = 0.000$; TLR4 (L816A)-EGFP/MD-2 (+), $p = 0.018$; and TLR4 (D817A)-EGFP/MD-2 (+), $p = 0.007$).

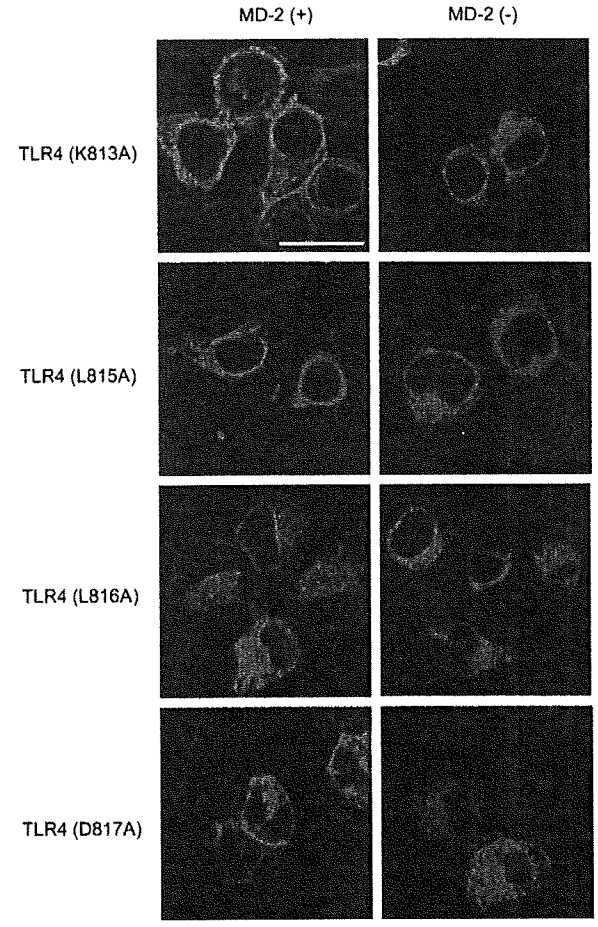


FIGURE 7. **Leucines at the position 815 and 816 of TLR4 are responsible for full plasma membrane expression.** Cells were cultured on coverslips in 12-well plates and transfected as in Fig. 2. EGFP-tagged TLR4 was visualized by laser confocal microscopy. Each genotype of TLR4-EGFP was cotransfected with human MD-2 plasmid or empty vector. *Bar*, 20 μm.

between EGFP-tagged proteins and FLAG-$His_6$-tagged proteins in the relative pattern of responsiveness against LPS stimulation (Fig. 8*A*). Because CD14 is also important for LPS recognition by TLR4, we examined the effect of CD14 coexpression on the phenotypic changes of the mutants (17, 18). Coexpression of CD14 did not change the phenotypes of wild-type TLR4, TLR4 (L815A), and TLR4 (L816A) in terms of LSP responsiveness (data not shown).

Cell surface expressions of the wild-type, L815A mutant, and L816A mutant TLR4-FLAG- $His_6$ fusion proteins were also examined. Live cells transfected with wild-type TLR4, the L815A mutant or the L816A mutant as well as human MD-2 and CD14 were biotinylated on the cell surface, and the biotinylated proteins were affinity-purified and subjected to Western blotting. Fig. 8*B* shows the marked difference in cell surface expression of wild-type and mutants L815A and L816A. Note that biotinylated proteins have additional residues on every amine of the extracellular domain, which leads to a band shift during electrophoresis. Although both mutants were detected far less than the wild-type on the cell surface, comparatively more L816A mutant was expressed on the plasma membrane than L815A mutant, and the amount of L815A mutant seemed to be negligible compared with the wild type. These results may clarify the ambiguity of the microscopic observation of TLR4 (L815A) and TLR4 (L816A). Plasma membrane expression of TLR4 was impaired when the leucine at 815 or 816 was replaced to alanine. But the leucine at 815 is more critical, and the mutant L816A may show the weaker phenotypic change.

To further investigate the characteristics of the TLR4 (L815A) mutant, we performed an immunoprecipitation assay of wild-type and mutant TLR4. Cells were transfected with a human MD-2-FLAG-$His_6$ expression vector and either the wild-type or the mutant (L815A) TLR4-EGFP expression vector. Anti-TLR4 monoclonal antibody (clone HTA125), anti-GFP polyclonal antibody, or anti-FLAG monoclonal antibody was added to the lysate and precipitated with Protein G-Sepharose beads. Collected proteins were eluted and subjected to Western blotting. The results are shown in Fig. 8*C*. TLR4 (L815A) was not immunoprecipitated with anti-TLR4 antibody (HTA125). HTA125 antibody was raised against TLR4-expressing cells (9) and recognizes the extracellular portion of TLR4. This result suggests that the amino acid replacement at position 815 may cause a change in the extracellular portion of TLR4 and/or that the replacement may also inhibit cell surface expression of the mutant protein. On the other hand, both wild-type TLR4-EGFP and mutant TLR4-EGFP were immunoprecipitated with anti-GFP polyclonal antibody, which recognized EGFP. However, of the two bands of TLR4, the heavier band seems to be somewhat faint in the mutant, whereas in the wild type the heavier band is at least as dense as the lighter one. TLR4 can be detected as two separate bands in a Western blot (19), especially under transient transfection conditions. The difference in proportion of the heavy and light bands between wild-type and mutant TLR4 may suggest that there is some difference in glycosylation. Furthermore, wild-type TLR4 was coprecipitated with MD-2-FLAG-$His_6$, but the mutant TLR4 could not be detected (Fig. 8*C*, *lanes 4* and *8*). Because MD-2 is

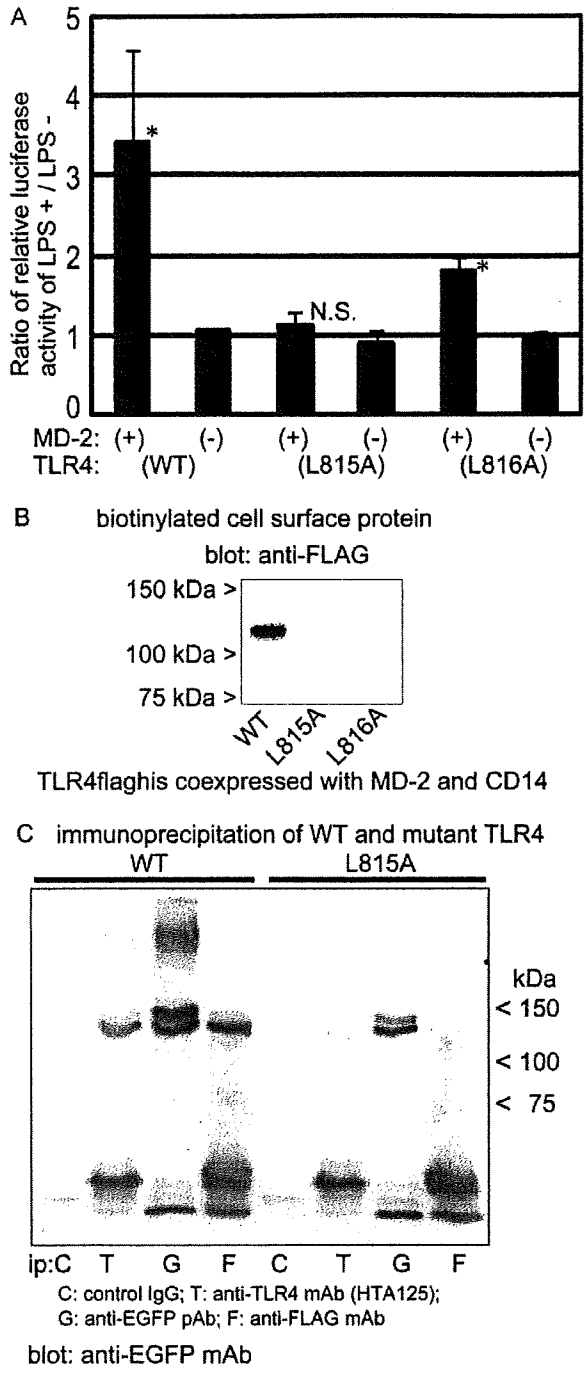


FIGURE 8. *A*, TLR4 mutants L815A and L816A with and without EGFP fusion exhibit the same phenotypes in LPS responsiveness and plasma membrane expression. HEK293T cells were transfected with the wild-type, the L815A or L816A mutant TLR4flaghis plasmid plus the human MD-2 plasmid and luciferase reporter, or control plasmids. After 36 h, cells were stimulated with LPS (10 ng/ml) for 7 h, and luciferase reporter gene activity was measured. The data were from three independent experiments. *Small bars* indicate 95% confidence intervals of the mean (*p* values for * are: TLR4 (WT) flaghis/MD-2 (+), $p = 0.046$; TLR4 (L816A) flaghis/MD-2 (+), $p = 0.003$). *N.S.*: not significant. *B*, wild-type and mutant TLR4s L815A and L816A were tagged by biotinylation of the cell surface proteins and affinity-purified. Human MD-2 and CD14 were coexpressed. TLR4 was visualized by immunoblotting using an anti-FLAG monoclonal antibody (*mAb*). Faint bands below 100 kDa are considered to be unbiotinylated intracellular TLR4 proteins that were not washed off during the process. Samples from TLR4 (WT), TLR4 (L815A), and TLR4 (L816A), respectively, were prepared from the same number of cells as for the biotinylation experiment. *C*, immunoprecipitation with antibodies further reveals the characteristics of TLR4 (L815A). Anti-TLR4 monoclonal antibody (HTA125) does not precipitate the mutant TLR4, whereas anti-GFP polyclonal antibody (*pAb*) precipitates both wild-type and mutant TLR4. Mutant TLR4 was not coprecipitated with MD-2-FLAG-$His_6$. Lysates were prepared from cells transiently expressing wild-type or mutant TLR4-EGFP and MD-2-FLAG-$His_6$.

associated with TLR4 (9), it is logical to expect that immunoprecipitating MD-2-FLAG-$His_6$ with anti-FLAG antibody should cause TLR4 to be coprecipitated with it. It is suggested by the result here that the association of the TLR4 mutant with MD-2 is impaired.

## DISCUSSION

In this research, we performed mutagenesis analyses of particular amino acid residues in TLR4 to explore the mechanisms of TLR4 intracellular signal transduction and subcellular distribution. We found the candidate residues by analyzing truncation mutants of TLR4 in the cytoplasmic region, in which both signaling and normal subcellular distribution of TLR4 are disturbed. Because we are focusing on a common mechanism for the impaired signaling and distribution, we finally picked a single amino acid mutant that does not respond to LPS stimuli, as measured with NF-κB reporter luciferase assay, and one that does not localize on the plasma membrane. TLR4 (L815A) is a mutant that meets these conditions, and our results suggest that the leucine at position 815 of TLR4 is required for both signal transduction and plasma membrane localization.

The best known single amino acid mutant of TLR4 is TLR4 (P712H) known as the *Lps*$^d$ mutation in the C3H/HeJ mouse, which corresponds to position 714 in this study of human TLR4 (5, 6, 20). Mice carrying this mutation opened up the rediscovery of TLR4 as a key player in innate immunity. Because this proline residue at this position is within the TIR domain and is conserved among TLRs or TLR4s of other species, it is assumed that the residue plays an important role in TLR4 function. The association of TLR4 (P712H) with its adapter proteins is reported to be intact, and the explanation for the functional impairment of TLR4 (P712H) is not clear (21–23).

Some single amino acid variants are found in humans, and these are related to the incidence or prognosis of some infections and other diseases. A growing body of data suggests that the ability of certain individuals to respond properly to TLR4 ligands may be impaired by single-nucleotide polymorphisms within TLR4 genes (24). The D299G and T399I alleles of the TLR4 gene have been associated with increased risk of severe infections (25).

By clarifying the subcellular component where the mutant protein is retained, or by clarifying to which compartment the mutant is not delivered, the abnormal intracellular sorting that is caused by the mutation in TLR4 (L815A) could be elucidated more precisely. Usually a sorting signal motif is comprised of several amino acids. In this regard, if the leucine at position 815 is a part of a motif, there should be other amino acids that are also members of the motif. Although replacement of leucine with alanine at position 816 did not cause an apparent signal transduction impediment, plasma membrane expression of TLR4 (L816A) was impaired to a certain extent. Positive

response to LPS stimulation by TLR4(L816A) could be attributable to this small amount of expression on the plasma membrane. Mutagenesis analyses of neighboring amino acids of the leucine at 815 were not definitive, but the results could be suggestive that the adjacent leucine at 816 may work together with the leucine at 815. Leucines at position 815 and 816 could be in the same motif, and the leucine at position 816 may be less critical.

Several proteins have been reported to be involved in TLR4 cell surface expression. Heat shock protein gp96 is necessary for TLR4 association with MD-2 in the ER and for subsequent cell surface expression (26). PRAT4A and PRAT4B are associated with TLR4 and regulate TLR4 cell surface expression (27, 28). In embryonic fibroblasts of MD-2 knockout mice, TLR4 localization on the cell surface is severely impaired, and most TLR4 is retained in the ER or Golgi apparatus (15). MD-2 binds to TLR4 at its extracellular domain and is essential for LPS recognition by TLR4 (29). Although proteins such as CD14 and LPS-binding protein are reported to have important roles in LPS recognition by TLR4, in an *in vitro* setting HEK293T cells gain LPS responsiveness by introducing only TLR4 and MD-2 genes when measured by NF-κB reporter assay (9, 30). Without transfection, HEK293 cells do not express TLR4, MD-2, or CD14, which are involved in LPS-induced intracellular signaling (31, 32). In this study, we show that the association of the TLR4 mutant and MD-2 is impaired (Fig. 8*C*).

Post-translational modification is another important factor for TLR4 function. Asparagine residues in the extracellular portion of TLR4 need to be glycosylated for plasma membrane expression of TLR4 (15, 19, 33). TLR4·MD-2 association is necessary for this glycosylation as well. The difference in the proportion of the heavy band to lighter band between wild-type and L815A mutant TLR4 immunoprecipitated with anti-GFP polyclonal antibody suggests that there may be some difference in glycosylation between wild-type and L815A mutant TLR4 (Fig. 8*C*). Although leucine at position 815 is located in the cytoplasmic tail of TLR4, we speculated that substitution of leucine at position 815 may cause a conformational change in the extracellular portion of the protein, which may interfere with the association between L815A mutant TLR4 and MD-2, leading to inhibition of glycosylation and cell surface expression of the mutant protein. Further investigation may reveal the mechanism involved in this phenotypic change in TLR4 (L815A), which would lead to better understanding of the mechanism of wild-type TLR4 signaling and trafficking.

*Acknowledgment—We greatly appreciate the gift of human TLR4 and MD-2 cDNA from Dr. Kensuke Miyake (Institute of Medical Science, University of Tokyo, Japan).*

## REFERENCES


1. Takeda, K., Kaisho, T., and Akira, S. (2003) *Annu. Rev. Immunol.* **21,** 335–376
2. Hoebe, K., Du, X., Georgel, P., Janssen, E., Tabeta, K., Kim, S. O., Goode, J., Lin, P., Mann, N., Mudd, S., Crozat, K., Sovath, S., Han, J., and Beutler, B. (2003) *Nature* **424,** 743–748
3. Oshiumi, H., Sasai, M., Shida, K., Fujita, T., Matsumoto, M., and Seya, T. (2003) *J. Biol. Chem.* **278,** 49751–49762
4. Yamamoto, M., Sato, S., Mori, K., Hoshino, K., Takeuchi, O., Takeda, K., and Akira, S. (2002) *J. Immunol.* **169,** 6668–6672
5. Qureshi, S. T., Lariviere, L., Leveque, G., Clermont, S., Moore, K. J., Gros, P., and Malo, D. (1999) *J. Exp. Med.* **189,** 615–625
6. Poltorak, A., He, X., Smirnova, I., Liu, M. Y., Van Huffel, C., Du, X., Birdwell, D., Alejos, E., Silva, M., Galanos, C., Freudenberg, M., Ricciardi-Castagnoli, P., Layton, B., and Beutler, B. (1998) *Science* **282,** 2085–2088
7. Visintin, A., Mazzoni, A., Spitzer, J. A., and Segal, D. M. (2001) *Proc. Natl. Acad. Sci. U. S. A.* **98,** 12156–12161
8. Nishitani, C., Mitsuzawa, H., Hyakushima, N., Sano, H., Matsushima, N., and Kuroki, Y. (2005) *Biochem. Biophys. Res. Commun.* **328,** 586–590
9. Shimazu, R., Akashi, S., Ogata, H., Nagai, Y., Fukudome, K., Miyake, K., and Kimoto, M. (1999) *J. Exp. Med.* **189,** 1777–1782
10. Bonifacino, J. S., and Traub, L. M. (2003) *Annu. Rev. Biochem.* **72,** 395–447
11. Nishimura, N., and Balch, W. E. (1997) *Science* **277,** 556–558
12. Nufer, O., and Hauri, H. P. (2003) *Curr. Biol.* **13,** R391–393
13. Slack, J. L., Schooley, K., Bonnert, T. P., Mitcham, J. L., Qwarnstrom, E. E., Sims, J. E., and Dower, S. K. (2000) *J. Biol. Chem.* **275,** 4670–4678
14. Latz, E., Visintin, A., Lien, E., Fitzgerald, K. A., Monks, B. G., Kurt-Jones, E. A., Golenbock, D. T., and Espevik, T. (2002) *J. Biol. Chem.* **277,** 47834–47843
15. Nagai, Y., Akashi, S., Nagafuku, M., Ogata, M., Iwakura, Y., Akira, S., Kitamura, T., Kosugi, A., Kimoto, M., and Miyake, K. (2002) *Nat. Immunol.* **3,** 667–672
16. Hein, C., and Andre, B. (1997) *Mol. Microbiol.* **24,** 607–616
17. Beutler, B. (2000) *Curr. Opin. Immunol.* **12,** 20–26
18. Akashi, S., Ogata, H., Kirikae, F., Kirikae, T., Kawasaki, K., Nishijima, M., Shimazu, R., Nagai, Y., Fukudome, K., Kimoto, M., and Miyake, K. (2000) *Biochem. Biophys. Res. Commun.* **268,** 172–177
19. Ohnishi, T., Muroi, M., and Tanamoto, K. (2003) *Clin. Diagn. Lab. Immunol.* **10,** 405–410
20. Xu, Y., Tao, X., Shen, B., Horng, T., Medzhitov, R., Manley, J. L., and Tong, L. (2000) *Nature* **408,** 111–115
21. Dunne, A., Ejdeback, M., Ludidi, P. L., O'Neill, L. A., and Gay, N. J. (2003) *J. Biol. Chem.* **278,** 41443–41451
22. Fitzgerald, K. A., Palsson-McDermott, E. M., Bowie, A. G., Jefferies, C. A., Mansell, A. S., Brady, G., Brint, E., Dunne, A., Gray, P., Harte, M. T., McMurray, D., Smith, D. E., Sims, J. E., Bird, T. A., and O'Neill, L. A. (2001) *Nature* **413,** 78–83
23. Horng, T., Barton, G. M., and Medzhitov, R. (2001) *Nat. Immunol.* **2,** 835–841
24. Schroder, N. W., and Schumann, R. R. (2005) *Lancet Infect. Dis.* **5,** 156–164
25. Agnese, D. M., Calvano, J. E., Hahm, S. J., Coyle, S. M., Corbett, S. A., Calvano, S. E., and Lowry, S. F. (2002) *J. Infect. Dis.* **186,** 1522–1525
26. Randow, F., and Seed, B. (2001) *Nat. Cell Biol.* **3,** 891–896
27. Wakabayashi, Y., Kobayashi, M., Akashi-Takamura, S., Tanimura, N., Konno, K., Takahashi, K., Ishii, T., Mizutani, T., Iba, H., Kouro, T., Takaki, S., Takatsu, K., Oda, Y., Ishihama, Y., Saitoh, S., and Miyake, K. (2006) *J. Immunol.* **177,** 1772–1779
28. Konno, K., Wakabayashi, Y., Akashi-Takamura, S., Ishii, T., Kobayashi, M., Takahashi, K., Kusumoto, Y., Saitoh, S., Yoshizawa, Y., and Miyake, K. (2006) *Biochem. Biophys. Res. Commun.* **339,** 1076–1082
29. Nishitani, C., Mitsuzawa, H., Sano, H., Shimizu, T., Matsushima, N., and Kuroki, Y. (2006) *J. Biol. Chem.* **281,** 38322–38329
30. Akashi, S., Shimazu, R., Ogata, H., Nagai, Y., Takeda, K., Kimoto, M., and Miyake, K. (2000) *J. Immunol.* **164,** 3471–3475
31. Espevik, T., Latz, E., Lien, E., Monks, B., and Golenbock, D. T. (2003) *Scand. J. Infect. Dis.* **35,** 660–664
32. Muta, T., and Takeshige, K. (2001) *Eur. J. Biochem.* **268,** 4580–4589
33. da Silva Correia, J., and Ulevitch, R. J. (2002) *J. Biol. Chem.* **277,** 1845–1854

Atherosclerosis 204 (2009) 619–623

Contents lists available at ScienceDirect

Atherosclerosis

journal homepage: www.elsevier.com/locate/atherosclerosis

# Association between metabolic syndrome and carotid atherosclerosis in individuals without diabetes based on the oral glucose tolerance test

Nobukazu Ishizaka[a,*], Yuko Ishizaka[b], Minoru Yamakado[b], Eiichi Toda[b], Kazuhiko Koike[c], Ryozo Nagai[a]

[a] Department of Cardiovascular Medicine, University of Tokyo, Graduate School of Medicine, Hongo 7-3-1 Bunkyo-ku, Tokyo 113-8655, Japan
[b] Center for Multiphasic Health Testing and Services, Mitsui Memorial Hospital, Tokyo, Japan
[c] Department of Infectious Diseases, University of Tokyo, Graduate School of Medicine, Tokyo, Japan

ARTICLE INFO

*Article history:*
Received 31 July 2008
Received in revised form 20 October 2008
Accepted 21 October 2008
Available online 30 October 2008

*Keywords:*
Metabolic syndrome
Carotid artery
Atherosclerosis
Risk factors
Glucose metabolism

ABSTRACT

*Introduction:* Whether or not metabolic syndrome is predictive of atherosclerotic disorders may depend on the population studied. We investigated whether metabolic syndrome is associated with carotid atherosclerosis in individuals who were shown not to have diabetes mellitus based on results of the 75-g oral glucose tolerance test (OGTT).
*Methods and results:* Between 1994 and 2003, 3904 individuals underwent general health screening that included the OGTT. Among these 3904 individuals, 3679 had a fasting plasma glucose of <126 mg/dL (subgroup 1), and 3488 had a 2-h post-OGTT glucose value of <200 mg/dL (subgroup 2). In both subgroups, metabolic syndrome was found to be a risk factor for carotid plaque and for carotid intima-media thickening in men, and tended to be a risk factor for carotid plaque in women after adjustment for age. Among 3473 individuals who had both a fasting plasma glucose value of <126 mg/dL and a 2-h post-OGTT glucose of <200 mg/dL, 2440 did not have hypertension, which was defined as systolic and diastolic blood pressure of <140/90 mmHg and absence of use of anti-hypertensive medication. In these non-diabetic non-hypertensive individuals, the association between metabolic syndrome and carotid plaque or carotid intima-media thickening was not statistically significant even with adjustment only for age.
*Conclusions:* In men who did not have impaired fasting glycemia and/or in those without impaired glucose tolerance, metabolic syndrome was a predictor of carotid atherosclerosis after age adjustment, although metabolic syndrome was not found to be a predictor of carotid atherosclerosis when hypertensive individuals were excluded from the study population.



## 1. Introduction

Metabolic syndrome (MetS) is a cluster of metabolic and hemodynamic abnormalities linked with insulin resistance. Since components of MetS also represent risk factors for atherosclerotic disorders, it is natural that individuals with this syndrome have an increased risk for ischemic heart disease [1] and stroke [2,3]. On the other hand, the clinical utility of MetS may depend on whether the risk conveyed by this syndrome is higher than the sum of each component utilized as diagnostic criteria for MetS [4,5].

Carotid artery intima-media thickness has been reported to be a discriminator as a surrogate of cardiovascular mortality in community-dwelling Japanese people [6] and, conversely, aggregation of established major coronary risk factors has been reported to strongly influence the presence of carotid atherogenesis in the general Japanese population [7]. Previously, we reported that the presence of MetS may not increase the risk for carotid atherosclerosis in individuals without hypertension, with hypertension defined as systolic blood pressure (SBP) of ≥140 mmHg, diastolic blood pressure (DBP) of ≥90 mmHg, or the use of anti-hypertensive medication [8]. This observation suggested that the properties of MetS that present a risk for atherosclerotic diseases may differ according to the populations selected. Consistent with this idea, it was reported that MetS was not found to be associated with cardiovascular mortality in non-diabetic non-hypertensive Chinese individuals [9], and that MetS did not significantly increase the risk of mortality from cardiovascular disease in non-diabetic Mexican Americans and non-Hispanic whites [10]. In the current study, we investigated whether MetS was associated with carotid atherosclerosis in Japanese individuals who did not have diabetes mellitus based on results of the 75-g oral glucose tolerance test (OGTT).

* Corresponding author. Tel.: +81 3 3815 5411x37156; fax: +81 3 5842 5586.
*E-mail address:* nobuishizka-tky@umin.ac.jp (N. Ishizaka).

0021-9150/$ – see front matter © 2008 Elsevier Ireland Ltd. All rights reserved.
doi:10.1016/j.atherosclerosis.2008.10.022

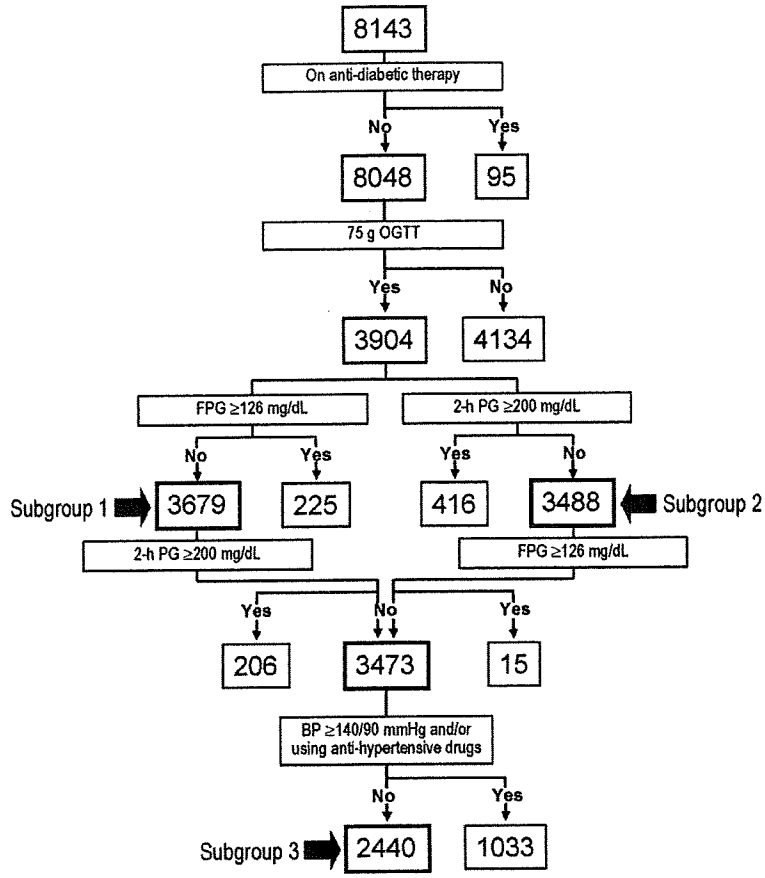


**Fig. 1.** Flow chart showing selection of the four subgroups.

## 2. Methods

### 2.1. Study subjects and selection of subgroups

The study was approved by The Ethical Committee of Mitsui Memorial Hospital and University of Tokyo, Faculty of Medicine. Between September 1994 and December 2003, 8143 subjects underwent general health screening including carotid ultrasonography at the Center for Multiphasic Health Testing and Services, Mitsui Memorial Hospital. Of the 8143 subjects, 95 were treated as having diabetes, and of the remaining 8048 individuals, 3904 underwent an OGTT. Among these 3904 individuals, three subgroups were sequentially selected based on various parameters (Fig. 1). Those with a fasting plasma glucose (FPG) value of <126 mg/dL were designated as subgroup 1, and those with a 2-h post-OGTT plasma glucose (2-h PG) value of <200 mg/dL were designated as subgroup 2. Subgroup 3 was comprised of subjects who met all the following conditions: FPG of <126 mg/dL, 2-h PG of <200 mg/dL, and not having hypertension. Hypertension was defined as SBP ≥140 mmHg, DBP ≥90 mmHg, or the use of anti-hypertensive medication. We also selected individuals without impaired glucose tolerance (IGT), i.e., individuals with a 2-h PG value of <140 mg/dL.

At our institute, several types of health screening programs are available, and some general health screening programs include carotid ultrasonography and/or OGTT, while others do not. However, the decision on the type of health screening was made by the individuals and/or their companies and was not decided upon or recommended by any attending physician.

### 2.2. Definition of MetS

MetS was defined as the presence of three or more of the following: (1) fasting glucose ≥110 mg/dL; (2) SBP/DBP ≥130/85 mmHg or taking anti-hypertensive medication; (3) triglycerides ≥150 mg/dL mmol/L; (4) HDL cholesterol <40 mg/dL in men and <50 mg/dL in women; and (5) body mass index ≥25 kg/m$^2$ [11].

### 2.3. Carotid ultrasonography

Carotid artery status was studied using high resolution B-mode ultrasonography (Sonolayer SSA270A, Toshiba, Japan) equipped with a 7.5 MHz transducer as described previously [12]. Plaque was defined to be present when there is one or more clearly isolated focal thickening(s) of the intima-media layer with thickness of ≥1.3 mm at the common or internal carotid artery or the carotid bulb. Carotid wall intima-media thickening was said to be present when intima-media thickness which was measured at the far wall of the distal 10 mm of the common carotid artery was ≥1.0 mm [12].

### 2.4. Statistical analysis

Logistic regression analysis was used to obtain adjusted odds ratios and their 95% confidence intervals (CIs) to predict the presence of carotid plaque or carotid intima-media thickening. Statistical analyses were carried out by using Dr. SPSS II (SPSS Inc., Chicago, IL). Results are expressed as the mean ± standard deviation (SD). A value of $p < 0.05$ was taken to be statistically significant.

**Table 1**
Baseline characteristics.

| Variables | Subgroup 1 | | Subgroup 2 | | Subgroup 3 | |
|---|---|---|---|---|---|---|
| | Men | Women | Men | Women | Men | Women |
| Number | 2548 | 1131 | 2386 | 1102 | 1588 | 852 |
| Age, years | 58.2 ± 10.6 | 57.9 ± 10.4 | 58.0 ± 10.7 | 57.8 ± 10.3 | 56.7 ± 10.9 | 56.6 ± 10.5 |
| Body mass index, kg/m$^2$ | 24.0 ± 2.8 | 22.2 ± 3.1 | 23.9 ± 2.7 | 22.1 ± 3.1 | 23.6 ± 2.6 | 21.7 ± 2.8 |
| Systolic BP, mmHg | 127 ± 19 | 121 ± 21 | 128 ± 19 | 120 ± 20 | 119 ± 12 | 123 ± 14 |
| Diastolic BP, mmHg | 79 ± 12 | 73 ± 12 | 79 ± 12 | 73 ± 12 | 73 ± 8 | 69 ± 9 |
| Total cholesterol, mg/dL | 206 ± 32 | 219 ± 35 | 205 ± 32 | 219 ± 35 | 205 ± 32 | 216 ± 35 |
| HDL-cholesterol, mg/dL | 55 ± 16 | 70 ± 17 | 55 ± 16 | 70 ± 17 | 56 ± 16 | 71 ± 17 |
| Triglycerides, mg/dL | 144 ± 117 | 96 ± 56 | 142 ± 98 | 95 ± 54 | 141 ± 98 | 95 ± 54 |
| Uric acid, mg/dL | 6.2 ± 1.2 | 4.7 ± 1.0 | 6.2 ± 1.2 | 4.7 ± 1.0 | 6.2 ± 1.2 | 4.6 ± 1.0 |
| Fasting glucose, mg/dL | 96 ± 10 | 90 ± 10 | 95 ± 10 | 90 ± 9 | 94 ± 9 | 88 ± 9 |
| 2-h OGTT glucose, mg/dL | 132 ± 41 | 118 ± 32 | 125 ± 29 | 115 ± 26 | 121 ± 29 | 112 ± 25 |
| Haemoglobin A1C, % | 5.2 ± 0.4 | 5.1 ± 0.4 | 5.2 ± 0.4 | 5.1 ± 0.4 | 5.2 ± 0.4 | 5.1 ± 0.4 |
| Hypertension, *n* (%) | 863 (34) | 263 (23) | 788 (33) | 248 (23) | 0 | 0 |
| Anti-hypertensive drugs, *n* (%) | 336(13) | 99(9) | 307(13) | 95(9) | 0 | 0 |
| Metabolic syndrome, *n* (%) | 439(17) | 84(7) | 372(16) | 72(7) | 131 (8) | 25(3) |
| Smoking status | | | | | | |
| Never, *n* (%) | 764 (30) | 933 (82) | 714(30) | 909 (82) | 465 (29) | 689(81) |
| Former, *n* (%) | 799(31) | 53(5) | 753 (32) | 50(5) | 464 (29) | 44(5) |
| Current, *n* (%) | 985 (39) | 145(13) | 919(39) | 143(13) | 659(41) | 119(14) |

BP indicates blood pressure, OGTT indicates oral glucose tolerance test.

## 3. Results

### *3.1. Association between MetS and carotid atherosclerosis in individuals with FPG value of <126 mg/dL (subgroup 1)*

Among the 3904 individuals who underwent OGTT, 3679 (94%) had an FPG value of less than 126 mg/dL. Of these, 300 (257 men, 43 women), the FPG value was ≥110 mg/dL, thus impaired fasting glycemia (IFG), and in the remaining 3379 (2291 men, 1088 women) had an FPG value of less than 110 mg/dL (no IFG). Table 1 shows the baseline characteristics of this group according to gender. Carotid plaque was found in 823 (32%) men and 191 (17%) women and carotid intima-media thickening was found in 422 (17%) men and 122 (11%) women (Fig. 2). Age-adjusted logistic regression analysis (Model 2) showed that, in men, MetS was statistically significantly associated with carotid plaque (Table 1) and intima-media thickening (Table 2). In women, MetS tended to be associated with carotid plaque, but not with intima-media thickening after age adjustment. Similar patterns of relationships could be observed after further adjustment for total cholesterol (TC) and smoking status (Model 3). On the other hand, after full adjustment including that for components of MetS (Model 4), MetS was not significantly associated with carotid plaque or intima-media thickening in either men or women.

### *3.2. Association between metabolic syndrome and carotid atherosclerosis in individuals with 2-h PG value of <200 mg/dL (subgroup 2)*

Among 3904 individuals who underwent OGTT, 3488 (89%) had a 2-h PG value of less than 200 mg/dL. Of these 3488 individuals 2644 (1717 men, 927 women) had a 2-h PG value of less than 140 mg/dL (no IGT) and the remaining 844 (669 men, 175 women) had a 2-h PG FPG value of ≥140 mg/dL, and thus IGT. Carotid plaque was found in 761 (32%) men and 182 (17%) women and carotid intima-media thickening was found in 378 (16%) men and 116 (11%) women. Age-adjusted logistic regression analysis (Model 2) showed that, in men, MetS was statistically significantly associated with carotid plaque (Table 2) and intima-media thickening (Table 3). In women, MetS tended to be associated with carotid plaque but not with intima-media thickening. Similar patterns of relationship could be observed after further adjustment for TC and smoking status (Model 3). On the other hand, after full adjustment that included components of MetS (Model 4), MetS was not significantly associated with carotid plaque or intima-media thickening in men or in women. There were only 15 (13 men, 2 women)

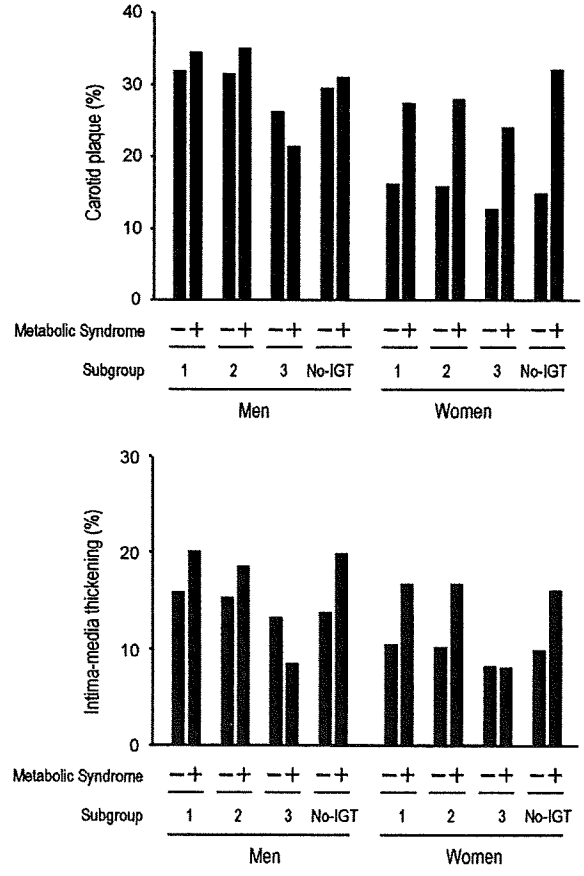


**Fig. 2.** Prevalence of carotid plaque and carotid intima-media thickening according to the presence or absence of metabolic syndrome in subgroups.

**Table 2**
Logistic regression analysis with metabolic syndrome as an independent variable and carotid plaque as a dependent variable.

| Variables | Odds ratio for carotid plaque | | | |
|---|---|---|---|---|
| | Men | | Women | |
| | Odds ratio (95% CI) | *P* value | Odds ratio (95% CI) | *P* value |
| *Subgroup 1* | | | | |
| Model 1 | 1.12(0.90–1.39) | 0.302 | 1.97(1.19–3.28) | 0.009 |
| Model 2 | 1.41(1.11–1.79) | 0.005 | 1.68(0.96–2.95) | 0.072 |
| Model 3 | 1.30(1.03–1.67) | 0.030 | 1.63(0.93–2.88) | 0.091 |
| Model 4 | 1.21(0.90–1.63) | 0.209 | 1.61(0.79–3.29) | 0.188 |
| *Subgroup 2* | | | | |
| Model 1 | 1.18(0.93–1.49) | 0.170 | 2.06(1.20–3.55) | 0.009 |
| Model 2 | 1.47(1.14–1.90) | 0.003 | 1.78(0.98–3.24) | 0.058 |
| Model 3 | 1.38(1.07–1.78) | 0.014 | 1.72(0.95–3.14) | 0.076 |
| Model 4 | 1.23(0.90–1.69) | 0.202 | 1.73(0.82–3.63) | 0.151 |
| *Subgroup 3* | | | | |
| Model 1 | 0.77(0.50–1.19) | 0.232 | 2.20(0.86–5.62) | 0.101 |
| Model 2 | 0.99(0.62–1.58) | 0.971 | 1.89(0.66–5.43) | 0.235 |
| Model 3 | 0.94(0.59–1.50) | 0.796 | 1.85(0.64–5.33) | 0.254 |
| Model 4 | 0.82(0.48–1.41) | 0.479 | 2.44(0.72–8.29) | 0.152 |

Model 1, unadjusted; Model 2, adjusted for age; Model 3, adjusted for age, total cholesterol and smoking status; Model 4, adjusted for age, body mass index, systolic blood pressure, total cholesterol, HDL cholesterol, triglycerides, fasting plasma glucose, and smoking status.

individuals among the 3488 in subgroup 2 who had an FPG value of <126 mg/dL in addition to a 2-h PG value of <200 mg/dL, and, thus, the mode of association between MetS, carotid plaque, and intima-media thickening in this subgroup was essentially the same as that observed in total population of subgroup 2.

We also investigated the association between MetS and carotid atherosclerosis in individuals without IGT. There were 2644 individuals who did not have IGT, and among them, 61 had FPG value of ≥110 mg/dL (Fig. 2, Supplementary Tables 1 and 2). The obtained results in these subgroups were similar to those in the subgroup 2; however, association between MetS and carotid intima-media thickening was statistically significant even after multivariate adjustment in women.

**Table 3**
Logistic regression analysis with metabolic syndrome as an independent variable and carotid intima-media thickening as a dependent variable.

| Variables | Odds ratio for carotid intima-media thickening | | | |
|---|---|---|---|---|
| | Men | | Women | |
| | Odds ratio (95% CI) | *P* value | Odds ratio (95% CI) | *P* value |
| *Subgroup 1* | | | | |
| Model 1 | 1.33(1.03–1.73) | 0.031 | 1.74(0.95–3.19) | 0.074 |
| Model 2 | 1.74(1.31–2.30) | <0.001 | 1.40(0.72–2.73) | 0.324 |
| Model 3 | 1.65(1.24–2.19) | <0.001 | 1.38(0.70–2.70) | 0.349 |
| Model 4 | 0.97(0.67–1.39) | 0.851 | 0.70(0.31–1.60) | 0.398 |
| *Subgroup 2* | | | | |
| Model 1 | 1.26(0.94–1.68) | 0.120 | 1.78(0.93–3.42) | 0.083 |
| Model 2 | 1.63(1.20–2.22) | 0.002 | 1.47(0.73–2.98) | 0.285 |
| Model 3 | 1.55(1.13–2.11) | 0.006 | 1.44(0.71–2.93) | 0.317 |
| Model 4 | 1.00(0.68–1.48) | 0.993 | 0.71(0.30–1.67) | 0.435 |
| *Subgroup 3* | | | | |
| Model 1 | 0.61(0.32–1.15) | 0.125 | 0.99(0.23–4.28) | 0.985 |
| Model 2 | 0.83(0.43–1.61) | 0.586 | 0.71(0.15–3.41) | 0.673 |
| Model 3 | 0.77(0.40–1.50) | 0.443 | 0.70(0.15–3.39) | 0.660 |
| Model 4 | 0.52(0.24–1.11) | 0.092 | 0.56(0.05–1.45) | 0.123 |

Model 1, unadjusted; Model 2, adjusted for age; Model 3, adjusted for age, total cholesterol and smoking status; Model 4, adjusted for age, body mass index, systolic blood pressure, total cholesterol, HDL cholesterol, triglycerides, fasting plasma glucose, and smoking status.

### *3.3. Association between metabolic syndrome and carotid atherosclerosis in individuals with FPG value of <126 mg/dL, 2-h PG value of <200 mg/dL, and no hypertension (subgroup 3)*

Among 3904 individuals who underwent OGTT, 2440 (63%) could be assigned to subgroups 3. Their baseline characteristics according to gender are shown in Table 1. Carotid plaque was found in 409 (26%) men and 110 (13%) women and carotid intima-media thickening was found in 202 (13%) men and 69 (8%) women. Unlike subgroups 1 and 2, MetS was not significantly associated with either carotid plaque or intima-media thickening after age adjustment, or even before any adjustment in either gender (Tables 2 and 3).

## 4. Discussion

Here, we have assessed whether MetS is a risk factor for carotid atherosclerosis in individuals who were determined not to have diabetes mellitus based on results of OGTT. MetS was found to be associated with carotid atherosclerosis especially in men; however, when individuals with hypertension, defined as those having SBP/DBP ≥140/90 mmHg or using anti-hypertensive medication, were excluded, the presence of MetS no longer conferred excess risk when adjustments were made only for age or even when no adjustments were made.

It is known that clustering of certain metabolic abnormalities and hypertension increases the incidence of atherosclerotic diseases [13]. However, whether such clustering of atherogenic risk factors should be separately designated as MetS has been controversial. Whether MetS is independently associated with carotid atherosclerosis has been analyzed in various populations. By analyzing data on a multi-ethnic cohort of apparently healthy individuals in Canada, Paras et al. reported that although MetS was significantly associated with measures of sub-clinical carotid atherosclerosis, this association is mediated entirely through the components of MetS that have been considered as risk factors [14]. Similarly, by analyzing data on individuals recruited from a local community in Italy, Fadini et al. demonstrated that the clustering of MetS components led to a no-more-than additive increase in carotid intima-media thickness [4]. In addition, Vaidya et al. reported that MetS did not have supra-additive association with carotid intima-media thickening [15].

In our previous study that analyzed data on subjects who underwent general health screening, we found that MetS may not be associated with carotid atherosclerosis even after adjustment only for age when individuals did not have hypertension (SBP/DBP <140/90 mmHg and not using anti-hypertensive medication) [8]. In the current study, we expanded this theme to investigate whether MetS increases the risk for carotid atherosclerosis in individuals who had no or only mild (i.e., not in the diabetic range) abnormalities in glucose metabolism. We found that in individuals with FPG values of <126 mg/dL (subgroup 1) or in those with 2-h PG values of <200 mg/dL (subgroup 2), MetS was positively associated with carotid plaque after adjustment for only age (Model 2), although the relationship was only borderline positive in women. In men, the association between MetS and carotid intima-media thickening was also statistically significantly positive after adjustment for only age. These associations lost statistical significance after adjustment for TC, smoking status, and components of MetS (Model 4), suggesting that these associations may not be independent of these factors. Attention should be given to the fact that after excluding individuals with hypertension from the analysis, the association between MetS and carotid plaque or carotid intima-media thickening was no longer statistically significant even after adjustment for only age (subgroup 3), which is in agreement with our previous finding [8].

Several previous cross-sectional and longitudinal studies have investigated whether MetS increases the risk for atherosclerotic diseases in subjects without apparent impairment in glucose metabolism. A prospective population-based study of Finnish men showed that MetS was associated with higher mortality from coronary heart disease in men without impaired fasting glycemia [16]. Wilson et al. reported that MetS was associated with increased risk for cardiovascular disease in those without diabetes [17]. Leoncini et al. reported that MetS was associated with carotid atherosclerosis in non-diabetic hypertensive individuals who attended an outpatient clinic in Italy [18]. Kawamoto et al. analyzed Japanese inpatients and found that MetS increased the risk for carotid intima-media thickening in non-diabetic subjects [19]. Tzou et al. reported that the presence of MetS increased the composite of carotid intima-media thickness of ≥75th percentile of enrolled subjects in non-diabetic young adults [20]. These results support the notion that the presence of MetS will increase the risk for carotid atherosclerosis even in non-diabetic populations; however, caution should be paid in interpreting these results, as these results were not always adjusted for each component of MetS. The present results showed that MetS was associated with carotid plaque and intima-media thickening in men in subgroups 1, and 2 after adjustment for age, TC, and smoking status, although statistically significance would be lost after further adjustment for MetS components.

We found that in the absence of hypertension (subgroup 3), the association between MetS and carotid plaque or intima-media thickening was no more statistically significant after adjustment for only age, or even when no adjustments were made. These data collectively suggested that the presence or absence of hypertension, but not an abnormality in glucose metabolism, is crucial to determine whether the presence of MetS would increase the risk for carotid atherosclerosis. A recent study showed that MetS significantly increased all-cause mortality in hypertensive community-based French individuals with a hazard ratio of 1.40 (95% CI 1.13–1.74), but not in non-hypertensive individuals, during a mean follow-up period of 4.7 years [21], which was consistent with the idea of major role played by hypertension.

This study has several limitations. First, due to the cross-sectional nature of the study, we cannot determine whether there is a causal or resultant relationship between the MetS and presence of atherosclerosis. Second, among 8048 individuals who were not taking anti-diabetic medication, we excluded 4144 individuals who did not undergo OGTT. The mean age of the 3904 individuals who underwent OGTT and those 4144 who did not were significantly different ($55 \pm 10$ years versus $58 \pm 10$ years, respectively, $P < 0.001$); therefore, it could be said that there had been some selection bias, though, again, the type of health screening was not decided or recommended by the physicians.

In conclusion, we showed that MetS was associated with carotid plaque and carotid intima-media thickening in non-diabetic individuals; although, this relationship did not remain statistically significant after adjustment for MetS components. In non-diabetic non-hypertensive individuals, the association between MetS and carotid plaque or carotid intima-media thickening was not statistically significant when adjustment was made for only age or even when no adjustment were made. These data collectively indicate that presence or absence of hypertension, but not an abnormality in glucose metabolism, is crucial to determine the relationship between MetS and carotid atherosclerosis.

## Acknowledgements

The work was supported in part by a grant from the Smoking Research Foundation, that from Chiyoda Mutual Life Foundation, from the St. Luke's Grant for the Epidemiological Research, and that from Daiwa Securities Health Foundation. We are highly appreciative of Kyoko Furuta for her excellent technical assistance.

## Appendix A. Supplementary data

Supplementary data associated with this article can be found, in the online version, at doi:10.1016/j.atherosclerosis.2008.10.022.

## References

[1] Iso H, Sato S, Kitamura A, et al. Metabolic syndrome and the risk of ischemic heart disease and stroke among Japanese men and women. Stroke 2007;38:1744–51.
[2] Kwon HM, Kim BJ, Lee SH, Choi SH, Oh BH, Yoon BW. Metabolic syndrome as an independent risk factor of silent brain infarction in healthy people. Stroke 2006;37:466–70.
[3] Wang J, Ruotsalainen S, Moilanen L, Lepisto P, Laakso M, Kuusisto J. The metabolic syndrome predicts incident stroke: a 14-year follow-up study in elderly people in Finland. Stroke 2008;39:1078–83.
[4] Fadini GP, Coracina A, Inchiostro S, Tiengo A, Avogaro A, de Kreutzenberg SV. A stepwise approach to assess the impact of clustering cardiometabolic risk factors on carotid intima-media thickness: the metabolic syndrome no-more-than-additive. Eur J Cardiovasc Prev Rehabil 2008;15:190–6.
[5] Kahn R, Buse J, Ferrannini E, Stern M. The metabolic syndrome: time for a critical appraisal: joint statement from the American Diabetes Association and the European Association for the Study of Diabetes. Diabetes Care 2005;28:2289–304.
[6] Murakami S, Otsuka K, Hotta N, et al. Common carotid intima-media thickness is predictive of all-cause and cardiovascular mortality in elderly community-dwelling people: Longitudinal Investigation for the Longevity and Aging in Hokkaido County (LILAC) study. Biomed Pharmacother 2005;59(Suppl 1):S49–53.
[7] Mannami T, Baba S, Ogata J. Strong and significant relationships between aggregation of major coronary risk factors and the acceleration of carotid atherosclerosis in the general population of a Japanese city: the Suita Study. Arch Intern Med 2000;160:2297–303.
[8] Ishizaka N, Ishizaka Y, Hashimoto H, et al. Metabolic syndrome may not associate with carotid plaque in subjects with optimal, normal, or high-normal blood pressure. Hypertension 2006;48:411–7.
[9] Hsu PF, Chuang SY, Cheng HM, et al. Clinical significance of the metabolic syndrome in the absence of established hypertension and diabetes: a community-based study. Diabetes Res Clin Pract 2008;79:461–7.
[10] Stern MP, Williams K, Hunt KJ. Impact of diabetes/metabolic syndrome in patients with established cardiovascular disease. Atheroscler Suppl 2005;6:3–6.
[11] Ishizaka N, Ishizaka Y, Toda E, Hashimoto H, Nagai R, Yamakado M. Association between cigarette smoking, metabolic syndrome, and carotid arteriosclerosis in Japanese individuals. Atherosclerosis 2005;181:381–8.
[12] Ishizaka N, Ishizaka Y, Takahashi E, et al. Association between insulin resistance and carotid arteriosclerosis in subjects with normal fasting glucose and normal glucose tolerance. Arterioscler Thromb Vasc Biol 2003;23:295–301.
[13] Fowkes FG, Murray GD, Butcher I, et al. Ankle brachial index combined with Framingham Risk Score to predict cardiovascular events and mortality: a meta-analysis. JAMA 2008;300:197–208.
[14] Paras E, Mancini GB, Lear SA. The relationship of three common definitions of the metabolic syndrome with sub-clinical carotid atherosclerosis. Atherosclerosis 2008;198:228–36.
[15] Vaidya D, Szklo M, Liu K, et al. Defining the metabolic syndrome construct: Multi-Ethnic Study of Atherosclerosis (MESA) cross-sectional analysis. Diabetes Care 2007;30:2086–90.
[16] Lakka HM, Laaksonen DE, Lakka TA, et al. The metabolic syndrome and total and cardiovascular disease mortality in middle-aged men. JAMA 2002;288:2709–16.
[17] Wilson PW, D'Agostino RB, Parise H, Sullivan L, Meigs JB. Metabolic syndrome as a precursor of cardiovascular disease and type 2 diabetes mellitus. Circulation 2005;112:3066–72.
[18] Leoncini G, Ratto E, Viazzi F, et al. Metabolic syndrome is associated with early signs of organ damage in nondiabetic, hypertensive patients. J Intern Med 2005;257:454–60.
[19] Kawamoto R, Tomita H, Ohtsuka N, Inoue A, Kamitani A. Metabolic syndrome, diabetes and subclinical atherosclerosis as assessed by carotid intima-media thickness. J Atheroscler Thromb 2007;14:78–85.
[20] Tzou WS, Douglas PS, Srinivasan SR, et al. Increased subclinical atherosclerosis in young adults with metabolic syndrome: the Bogalusa Heart Study. J Am Coll Cardiol 2005;46:457–63.
[21] Pannier B, Thomas F, Bean K, et al. The metabolic syndrome: similar deleterious impact on all-cause mortality in hypertensive and normotensive subjects. J Hypertens 2008;26:1223–8.

J Gastroenterol 2009; 44[Suppl XIX]:82–88
DOI 10.1007/s00535-008-2276-4

Journal of Gastroenterology



# Steatosis, liver injury, and hepatocarcinogenesis in hepatitis C viral infection

KAZUHIKO KOIKE

Department of Infectious Diseases, Internal Medicine, Graduate School of Medicine, University of Tokyo, 7-3-1 Hongo, Bunkyo-ku, Tokyo 113-8655, Japan

In addition to the link with development of hepatocellular carcinoma (HCC), hepatitis C virus (HCV) infection is associated with several hepatic and extrahepatic manifestations. A role of hepatic steatosis in the pathogenesis of chronic hepatitis C has been shown, implying hepatitis C as a metabolic disease. Furthermore, recent epidemiological studies have suggested a linkage between insulin resistance and chronic HCV infection. In addition to the data indicating the presence of lipid metabolism disturbance and insulin resistance in the cohort of chronic hepatitis C patients, we found evidence showing the association between these two conditions and HCV infection using mice transgenic for the HCV core gene. These mice develop HCC late in life after the phase of hepatic steatosis and insulin resistance. The nonappearance of both steatosis and HCC in HCV core gene transgenic mice that are null for the proteasome activator 28γ implies a close relationship between lipid metabolism disturbance and hepatocarcinogenesis. Also, the core protein is shown to bind with retinoid X receptor (RXR)-α, resulting in the upregulation of some lipid metabolism enzymes, including cellular retinol binding protein II and acyl-CoA oxidase. In addition, the persistent activation of peroxisome proliferator activated receptor (PPAR)-α has recently been found in the liver of HCV core gene transgenic mice, yielding dramatic changes in lipid metabolism and hepatocyte proliferation, including HCC development. These results would provide a clue for further understanding of the role of lipid metabolism in pathogenesis of HCV infection, including liver injury and hepatocarcinogenesis.

Received: June 9, 2008 / Accepted: August 10, 2008
*Reprint requests to:* K. Koike

**Key words:** lipid metabolism, transgenic mouse, oxidative stress, intracellular signal transduction, peroxisome proliferator activated receptor

## Introduction

Worldwide, approximately 170 million people are persistently infected with hepatitis C virus (HCV), which induces a spectrum of chronic liver diseases from chronic hepatitis to cirrhosis and, eventually, to hepatocellular carcinoma (HCC).[1] HCV has been given increasing attention because of its wide and deep penetration in the community, tied with a very high incidence of HCC in persistent HCV infection. Once liver cirrhosis is established in hosts persistently infected with HCV, HCC develops at a yearly rate of approximately 7%,[2] resulting in the development of HCC in nearly 90% of HCV-associated cirrhotic patients in 15 years. In addition, the outstanding features in the mode of hepatocarcinogenesis in HCV infection, i.e., development of HCC in a multicentric fashion and at a very high incidence, are not common in other malignancies except for hereditary cancers such as familial polyposis of the colon. Knowledge of the mechanism underlying HCC development in persistent HCV infection, therefore, is imminently required for the prevention of HCC.

In addition to the link with development of HCC, HCV infection is associated with several hepatic and extrahepatic manifestations.[3] A role of hepatic steatosis in the pathogenesis of chronic hepatitis C has been shown, implicating hepatitis C as a metabolic disease.[4] Moreover, recent epidemiological studies have suggested a linkage between insulin resistance and chronic HCV infection.[5] In addition to the epidemiological data indicating the presence of lipid metabolism disturbance and insulin resistance in the cohort of chronic hepatitis C patients, detailed analyses on the relationship between

metabolic disorders and chronic hepatitis C have revealed evidence showing a close association between the progression of liver fibrosis and metabolic abnormalities in HCV infection.[6] However, it is unclear yet whether a causative relationship exists between these medical conditions. Moreover, it is unclear whether such metabolic disorders contribute to hepatocarcinogenesis in HCV infection.

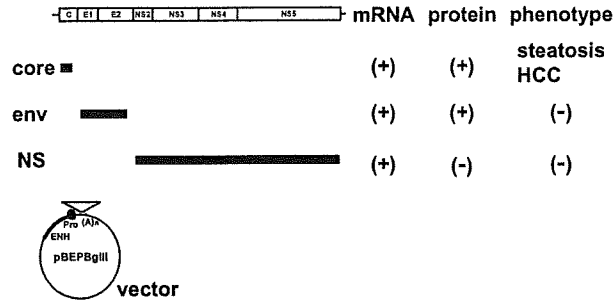


**Fig. 1.** Transgenic mouse lines carrying the hepatitis C virus (HCV) genome. Three different kinds of transgenic mouse lines, carrying the *core* gene, envelope genes, or nonstructural genes of HCV, respectively, were established under the control of the same regulatory elements. Among these mouse strains, only the transgenic mice carrying the HCV core gene develop hepatocellular carcinoma (HCC) after an early phase with hepatic steatosis in two independent lineages. The mice transgenic for the envelope genes or nonstructural genes do not develop HCC. *HCC*, hepatocellular carcinoma; *env*, envelope genes; *NS*, nonstructural genes

## Possible roles of HCV in hepatocarcinogenesis

The mechanism underlying hepatocarcinogenesis in HCV infection is not yet fully understood, despite the fact that nearly 80% of patients with HCC in Japan are persistently infected with HCV.[1,7,8] HCV infection is also common in patients with HCC in other countries, albeit to a lesser extent. These lines of evidence prompted us to seek to determine the role of HCV in hepatocarcinogenesis. Inflammation induced by HCV should be considered, of course, in a study on the hepatocarcinogenesis in hepatitis viral infection: necrosis of hepatocytes caused by chronic inflammation followed by regeneration enhances genetic aberrations in host cells, the accumulation of which culminates in HCC. This theory presupposes an indirect involvement of hepatitis viruses in HCC via hepatic inflammation. However, this context leaves us with a serious question: can inflammation alone result in the development of HCC in such a high incidence (90% in 15 years) or multicentric nature in HCV infection?

The other role of HCV would have to be weighed against an extremely rare occurrence of HCC in patients with autoimmune hepatitis in which severe inflammation in the liver persists indefinitely, even after the development of cirrhosis. This background and reasoning lead to a possible activity of viral proteins for inducing neoplasia. This possibility has been evaluated by introducing genes of HCV into hepatocytes in culture with little success. One of the difficulties in using cultured cells is the carcinogenic capacity of HCV, if any, which would be weak and would take a long time to manifest. Actually, it takes 30–40 years for HCC to develop in individuals infected with HCV. On the basis of these points of view, we started to investigate carcinogenesis in chronic hepatitis C, in vivo, by transgenic mouse technology.

## HCV core protein has an in vivo oncogenic activity as revealed by animal studies

Transgenic mouse lines carrying the HCV genome were engineered by introducing the genes from the cDNA of the HCV genome of genotype 1b.[9,10] Established are three different kinds of transgenic mouse lines, which carry the core gene, envelope genes, or nonstructural genes, respectively, under the same transcriptional regulatory element. Among these mouse lines, only the transgenic mice carrying the core gene developed HCC in two independent lineages.[10] The envelope gene transgenic mice do not develop HCC, despite high expression levels of both E1 and E2 proteins,[11,12] and the transgenic mice carrying the entire nonstructural genes have developed no HCC (Fig. 1).

The core gene transgenic mice express the core protein of an expected size, and the level of the core protein in the liver is similar to that in chronic hepatitis C patients. Early in life, these mice develop hepatic steatosis, which is one of the histological characteristics of chronic hepatitis C, along with lymphoid follicle formation and bile duct damage.[13] Thus, the core gene transgenic mouse model reproduces well the features of chronic hepatitis C. Of note, no pictures of significant inflammation are observed in the liver of this animal model. Late in life, these transgenic mice develop HCC. Notably, the development of steatosis and HCC has been reproduced by other HCV transgenic mouse lines, which harbor the entire HCV genome or structural genes including the core gene.[14–16] These outcomes indicate that the core protein, per se, of HCV has an oncogenic potential when expressed in vivo.

**Oxidative stress overproduction and intracellular signaling pathway activation are the major pathways in the core-induced liver pathology**

It is difficult to elucidate the mechanism underlying the development of HCC, even for our simple model in which only the core protein is expressed in otherwise normal liver. There is a notable feature in the localization of the core protein in hepatocytes; while the core protein predominantly exists in the cytoplasm associated with lipid droplets, it is also present in the mitochondria and nuclei.[10,17] On the basis of this finding, the pathways related to these two organelles, the mitochondria and nuclei, were thoroughly investigated.

One effect of the core protein is an increased production of oxidative stress in the liver. We would like to draw particular attention to the fact that the production of oxidative stress is increased in our transgenic mouse model in the absence of inflammation in the liver. This finding reflects a state of overproduction of reactive oxygen species (ROS) in the liver,[18] or predisposition to it, which is staged by the HCV core protein without any intervening inflammation.[19,20] The overproduction of oxidative stress results in the generation of deletions in mitochondrial and nuclear DNA, an indicator of genetic damage. In addition, analysis of antioxidant system revealed that some antioxidative molecules are not increased despite the overproduction of ROS in the liver of core gene transgenic mice: hemeoxygenase-1 and glutathione peroxidase are not augmented whereas catalase and glutathione S-transferase levels are increased and enhanced by iron overloading (Moriya et al., manuscript in preparation). These results suggest that HCV core protein not only induces overproduction of ROS but also attenuates some of the antioxidant systems, which may explain the mechanism underlying the production of a strong oxidative stress in HCV infection compared to other forms of hepatitis.

In the absence of inflammation, thus, the core protein induces oxidative stress overproduction, which may, at least in part, contribute to hepatocarcinogenesis in HCV infection. If inflammation were added to the liver with the HCV core protein, the production of oxidative stress would be escalated to an extent that can no longer be scavenged by a physiological antagonistic system. This idea suggests that the inflammation in chronic HCV infection would have a characteristic difference in its quality from those of other types of hepatitis, such as autoimmune hepatitis. The basis for the overproduction of oxidative stress may be ascribed to the mitochondrial dysfunction.[10,19] The dysfunction of the electron transfer system of the mitochondrion is suggested in association with the presence of the HCV core protein.[21]

Other pathways in hepatocarcinogenesis would be the alteration of the expression of cellular genes and modulation of intracellular signaling pathways. For example, tumor necrosis factor (TNF)-α and interleukin-1β have been found to be transcriptionally activated.[22] The mitogen-activated protein kinase (MAPK) cascade is also activated in the liver of the core gene transgenic mouse model. The MAPK pathway, which consists of three routes, c-Jun N-terminal kinase (JNK), p38, and extracellular signal-regulated kinase (ERK), is involved in numerous cellular events including cell proliferation. In the liver of the core gene transgenic mouse model before HCC development, only the JNK route is activated. Downstream of JNK activation, transcription factor activating protein (AP)-1 activation is markedly enhanced.[20,21] At far downstream, both the mRNA and protein levels of cyclin D1 and CDK4 are increased. Thus, the HCV core protein modulates the intracellular signaling pathways and gives an advantage for cell proliferation to the hepatocytes. Interestingly, we found recently that a protein interacting with the core protein, proteasome activator 28γ (PA28γ), is indispensable for the core protein to exert its function for the development of steatosis, insulin resistance, and HCC.[23,24]

**Lipid metabolism and HCV infection**

Steatosis is frequently observed in chronic hepatitis C patients and is significantly associated with increased fibrosis and progression rate of fibrosis of the liver.[6] A comprehensive analysis of gene expression in the liver of core gene transgenic mice, in which steatosis develops from early in life, revealed that a number of genes related to lipid metabolism are significantly upregulated or downregulated (Table 1).

The composition of fatty acids that are accumulated in the liver of core gene transgenic mice is different from that in fatty liver resulting from simple obesity. Carbon-18 monounsaturated fatty acids (C18:1) such as oleic or vaccenic acids are significantly increased; this is also the case in the comparison of liver tissues from hepatitis C patients and patients with simple fatty liver due to obesity.[20] The mechanism of steatogenesis in hepatitis C was investigated using this mouse model. There are at least three pathways for the development of steatosis. One is the frequent presence of insulin resistance in hepatitis C patients as well as in the core gene transgenic mice, which occurs through the inhibition of tyrosine phosphorylation of insulin receptor substrate (IRS)-1.[25] Insulin resistance increases the peripheral release and hepatic uptake of fatty acids, resulting in an accumulation of lipid in the liver. The second pathway is the suppression of the activity of

**Table 1.** Cellular genes differentially expressed in hepatitis C virus (HCV) core transgenic mouse liver

| | Upregulated | Downregulated |
|---|---|---|
| Lipid metabolism | NPC1 | Stearoyl-CoA desaturase |
| | Catalase | Sterol-carrier protein X |
| | Very long chain acyl-CoA dehydrogenase | Alpha-enolase carnitine acetyltransferase |
| | Carboxylesterase selenoprotein P | Gal beta 1,4(3) GlcNAc alpha 2,3-sialyltransferase |
| | Carbonic anhydrase | Very long chain acyl-CoA synthetase |
| | Adipose differentiation-related protein | Liver transferrin |
| | Bilirubin/phenol family UDP glucuronosyltransferase | 4-Hydroxyphenylpyruvate dioxygenase |
| | | LAF1 transketolase |
| | | *s*-Adenosylmethionine synthetase |
| | | Apolipoprotein A-II |
| Transcription and cell proliferation | Int-6 | Human guanine nucleotide regulatory protein |
| | GCN5L1 | Alpha-fetoprotein |
| | *H. sapiens* 8.2k-Da differentiation factor | Retinol binding protein |
| | USF1 | |
| | Initiation factor eIF-4AI | |
| | Human elongation factor-1-delta | |
| | Sui1 | |
| Inflammation | Alpha-1 protease inhibitor 3 | Alpha-2-macroglobulin |
| | Hemopexin | LMW prekininogen |
| | | Complement component C3 |
| | | AHSG(alpha 2 HS-glycoprotein) homologue |
| Others | Microvascular endothelial differentiation gene 1 | Vitronectin |
| | Diazepam-binding inhibitor | Epithelin 1 and 2 |
| | Argininosuccinate synthetase | Murinoglobulin |
| | Skeletal muscle alpha-tropomyosin | |
| | Ampd3 gene | |
| | DNA-binding protein | |

microsomal triglyceride transfer protein (MTP) by HCV core protein[26]; this inhibits the secretion of very low density protein (VLDL) from the liver, yielding an increase of triglycerides in the liver. The last pathway involves sterol regulatory element-binding protein (SREBP)-1c, which regulates the production of triglycerides and phospholipids. In HCV core gene transgenic mice, SREBP-1c is activated, whereas neither SREBP-2 nor SREBP-1a is upregulated.[27]

In relation to lipid metabolism, the core protein has also been found to interact with retinoid X receptor (RXR)-α.[28] RXR-α is one of the nuclear receptors, which forms a homodimer or heterodimers with other nuclear receptors, including PPAR (peroxisome proliferator-activated receptor)-α, and plays a pivotal role in the regulation of the expression of genes relating to lipid metabolism, cell differentiation, and proliferation. In fact, the core protein of HCV activates genes that have an RXR-α-responsive element as well as those with a PPAR-α-responsive element, both in mice and in cultured cells.[28] Based on these results, we, then, examined the expression and function of PPAR-α in the liver of core gene transgenic mice.

## PPAR-α activation in HCV-associated hepatocarcinogenesis

PPAR-α, one of the PPAR genes, plays a central role as a heterodimer with RXR-α in regulating fatty acid transport and catabolism. It is also known as a molecular target for lipid-lowering fibrate drugs.[29] On the other hand, prolonged administration of PPAR-α agonists causes HCC in rodents. Currently, there is little evidence that the low-affinity fibrate ligands are associated with human cancers, but it is possible that chronic activation of high-affinity ligands could be carcinogenic in humans.[29]

The level of PPAR-α protein was increased in the liver of core gene transgenic mice as early as 9 months of age. PPAR-α protein is accumulated with age in the nuclei of hepatocytes together with cyclin D1 protein. However, the level of PPAR-α mRNA was not increased at any age. By pulse-chase experiment, the stability of nuclear PPAR-α was increased in the presence of the core protein. In line with the increase of PPAR-α protein, target genes of PPAR-α were activated in the liver of core gene transgenic mice; these genes include

cyclin D1, cyclin-dependent kinase (CDK)-4, acy-CoA oxidase, and peroxisome thiolase.[30] However, in general, the activation of PPAR-α leads to improvement but not aggravation of steatosis. Then, what is the function of PPAR-α activation that is observed in the core gene transgenic mice?

To clarify the role of PPAR-α activation in pathogenesis of steatosis and HCC, we mated a core gene transgenic mouse with a PPAR-α knockout (KO) mouse and studied the phenotype. PPAR-α KO mice have reduced expression of target genes of PPAR-α, and have mild steatosis in the liver, as expected.[31] It was unanticipated, however, that steatosis was absent in PPAR-α-null or -heterozygous core gene transgenic mice but present in PPAR-α-intact core gene transgenic mice at the age of 9 or 24 months.[30] 8-Hydroxy deoxyguanosine (8-OHdG) and peroxylipids, both of which are markers for oxidative stress, were decreased in PPAR-α KO core gene transgenic mice. Mitochondrial dysfunction in the core gene transgenic mice, which contributes to overproduction of oxidative stress,[19] was also improved in PPAR-α KO core gene transgenic mice.

Finally, PPAR-α KO core gene transgenic mice did not develop HCC at the age of 24 months, whereas about one-third of PPAR-α-intact core gene transgenic mice did. It should be noted that core gene transgenic mice that are heterozygous for the PPAR-α gene also did not develop HCC.[32] When clofibrate, a peroxisome proliferator, was administered for 24 months to PPAR-α-heterozygous mice, either with or without the core gene, HCC developed in a higher rate in the core gene (+) mice with greater PPAR-α activation. It should be noted that steatosis was present only in core gene (+) PPAR-α-heterozygous mice. In summary, steatosis and HCC developed in PPAR-α-intact but not in PPAR-α-heterozygous or PPAR-α-null core gene transgenic mice, indicating that not the presence but the persistent activation of PPAR-α would be important in hepatocarcinogenesis by HCV core protein. In general, PPAR-α acts to ameliorate steatosis, but with the presence of mitochondrial dysfunction, which is also provoked by the core protein, the core-activated PPAR-α may exacerbate steatosis. Persistent activation of PPAR-α with "strong" ligands such as the core protein of HCV could be carcinogenic in humans, although the low-affinity fibrate ligands are not likely associated with human cancers.

### HCV core protein causes "fatty acid spiral"

Figure 2 illustrates our current hypothesis for the role of lipid metabolism in HCV-associated hepatocarcinogenesis. Immune-mediated inflammation should also play a pivotal role in hepatocarcinogenesis in HCV infection. However, in HCV infection, the core protein induces steatosis through the aforementioned pathways, leading to "fatty acid spiral" in the presence of the mitochondrial complex 1 dysfunction and PPAR-α activation, both of which are caused by the core protein. These intracellular alterations would contribute to hepatocarcinogenesis by inducing oxidative stress overproduction and cell-growth signal activation. In such a sense, the core protein of HCV is not a classical-type oncoprotein, but rather seems to contribute to hepatocarcinogenesis by modulating intracellular metabolism and signaling.

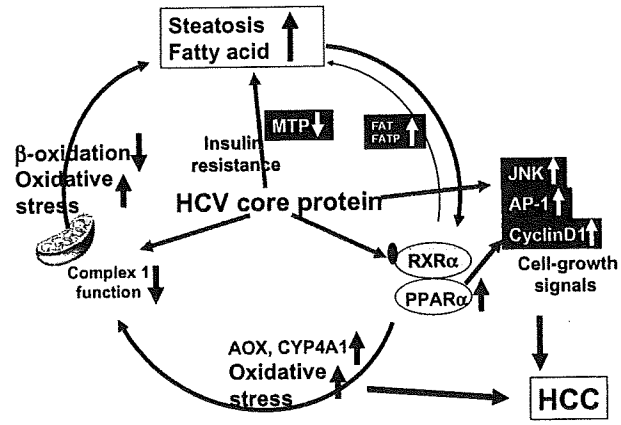


**Fig. 2.** "Fatty acid spiral" by HCV core protein. In HCV infection, the core protein induces steatosis via several pathways, leading to "fatty acid spiral" in the presence of the mitochondrial complex 1 dysfunction and PPAR-α activation, both of which are also caused by the core protein. These intracellular alterations would contribute to hepatocarcinogenesis by inducing oxidative stress overproduction and cell-growth signal activation. In such a sense, the core protein of HCV is not a classical type oncoprotein, but rather seems to contribute to hepatocarcinogenesis by modulating intracellular metabolism and signaling. *HCV*, hepatitis C virus; *HCC*, hepatocellular carcinoma; *ROS*, reactive oxygen species; *JNK*, c-Jun N-terminal kinase; *ERK*, extracellular signal-regulated kinase; *AP-1*, activating protein-1; *RXR-α*, retinoid X receptor-α; *PPAR-α*, peroxisome proliferator activated receptor-α; *AOX*, acyl-CoA oxidase; *CYP*, cytochrome P450; *MTP*, microsomal triglyceride transfer protein; *FAT*, fatty acid translocase; fatty acid transport protein

### The HCV protein may allow some steps in multistep hepatocarcinogenesis to be skipped

The results of our studies on transgenic mice have indicated a carcinogenic potential of the HCV core protein in vivo; thus, HCV would be directly involved in hepatocarcinogenesis. In research studies of carcinogenesis, the theory outlined by Kinzler and Vogelstein[33] has gained wide popularity. They have proposed that the

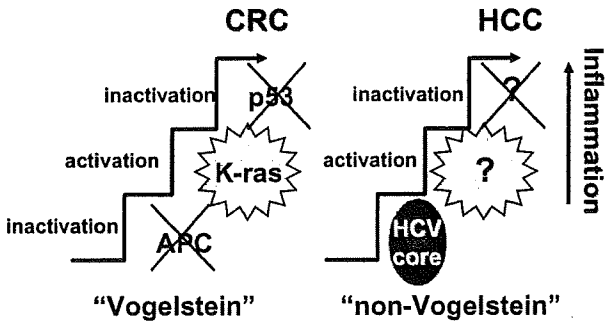


**Fig. 3.** Mechanism of HCV-associated hepatocarcinogenesis. Multiple steps are required in the induction of all cancers; it would be mandatory for hepatocarcinogenesis that genetic mutations accumulate in hepatocytes. However, in HCV infection, some of these steps may be skipped in the development of HCC in the presence of the core protein. The overall effects achieved by the expression of the core protein would be the induction of HCC, even in the absence of a complete set of genetic aberrations required for carcinogenesis. By considering such a "non-Vogelstein-type" process for the induction of HCC, a plausible explanation may be given for many unusual events happening in HCV carriers

development of colorectal cancer is induced by the accumulation of a complete set of cellular gene mutations. They have deduced that mutations in the APC gene for inactivation, those in K-*ras* for activation, and those in the p53 gene for inactivation accumulate, which cooperate toward the development of colorectal cancer.[33] Their theory has been extended to the carcinogenesis of other cancers as well, called "Vogelstein-type" carcinogenesis (Fig. 3).

On the basis of the results we obtained for the induction of HCC by the HCV core protein, we would like to introduce a different mechanism for hepatocarcinogenesis in HCV infection. We do allow multistages in the induction of all cancers; it would be mandatory for hepatocarcinogenesis that many mutations accumulate in hepatocytes. Some of these steps, however, may be skipped in the development of HCC in HCV infection to which the core protein would contribute (see Fig. 3). The overall effect achieved by the expression of the viral protein would be the induction of HCC, even in the absence of a complete set of genetic aberrations required for carcinogenesis.

By considering such a "non-Vogelstein-type" process for the induction of HCC, a plausible explanation may be given for many unusual events happening in HCV carriers.[34] Now it does not seem so difficult as before to determine why HCC develops in persistent HCV infection at an outstandingly high incidence. Our theory may also give an account of the nonmetastatic and multicentric de novo occurrence characteristics of HCC, which would be the result of persistent HCV infection.

## References


1. Saito I, Miyamura T, Ohbayashi A, Harada H, Katayama T, Kikuchi S, et al. Hepatitis C virus infection is associated with the development of hepatocellular carcinoma. Proc Natl Acad Sci USA 1990;87:6547–9.
2. Ikeda K, Saitoh S, Suzuki Y, Kobayashi M, Tsubota A, Koida I, et al. Disease progression and hepatocellular carcinogenesis in patients with chronic viral hepatitis: a prospective observation of 2215 patients. J Hepatol 1998;28:930–8.
3. Okuse C, Yotsuyanagi H, Koike K. Hepatitis C as a systemic disease: virus and host immunologic responses underlie hepatic and extrahepatic manifestations. J Gastroenterol 2007;42:857–65.
4. Koike K, Moriya K. Metabolic aspects of hepatitis C: steatohepatitis distinct from NASH. J Gastroenterol 2005;40:329–36.
5. Negro F. Insulin resistance and HCV: will new knowledge modify clinical management? J Hepatol 2006;45:514–9.
6. Powell EE, Jonsson JR, Clouston AD. Steatosis: co-factor in other liver diseases. Hepatology 2005;42:5–13.
7. Kiyosawa K, Sodeyama T, Tanaka E, Gibo Y, Yoshizawa K, Nakano Y, et al. Interrelationship of blood transfusion, non-A, non-B hepatitis and hepatocellular carcinoma: analysis by detection of antibody to hepatitis C virus. Hepatology 1990;12:671–5.
8. Yotsuyanagi H, Shintani Y, Moriya K, Fujie H, Tsutsumi T, Kato T, et al. Virological analysis of non-B, non-C hepatocellular carcinoma in Japan: frequent involvement of hepatitis B virus. J Infect Dis 2000;181:1920–8.
9. Moriya K, Yotsuyanagi H, Shintani Y, Fujie H, Ishibashi K, Matsuura Y, et al. Hepatitis C virus core protein induces hepatic steatosis in transgenic mice. J Gen Virol 1997;78:1527–31.
10. Moriya K, Fujie H, Shintani Y, Yotsuyanagi H, Tsutsumi T, Matsuura Y, et al. Hepatitis C virus core protein induces hepatocellular carcinoma in transgenic mice. Nat Med 1998;4:1065–8.
11. Koike K, Moriya K, Ishibashi K, Matsuura Y, Suzuki T, Saito I, et al. Expression of hepatitis C virus envelope proteins in transgenic mice. J Gen Virol 1995;76:3031–8.
12. Koike K, Moriya K, Yotsuyanagi H, Shintani Y, Fujie H, Ishibashi K, et al. Sialadenitis resembling Sjögren's syndrome in mice transgenic for hepatitis C virus envelope genes. Proc Natl Acad Sci USA 1997;94:233–6.
13. Bach N, Thung SN, Schaffner F. The histological features of chronic hepatitis C and autoimmune chronic hepatitis: a comparative analysis. Hepatology 1992;15:572–7.
14. Lerat H, Honda M, Beard MR, Loesch K, Sun J, Yang Y, et al. Steatosis and liver cancer in transgenic mice expressing the structural and nonstructural proteins of hepatitis C virus. Gastroenterology 2002;122:352–65.
15. Naas T, Ghorbani M, Alvarez-Maya I, Lapner M, Kothary R, De Repentigny Y, et al. Characterization of liver histopathology in a transgenic mouse model expressing genotype 1a hepatitis C virus core and envelope proteins 1 and 2. J Gen Virol 2005;86:2185–96.
16. Machida K, Cheng KT, Lai CK, Jeng KS, Sung VM, Lai MM. Hepatitis C virus triggers mitochondrial permeability transition with production of reactive oxygen species, leading to DNA damage and STAT3 activation. J Virol 2006;80:7199–207.
17. Moriya K, Fujie H, Yotsuyanagi H, Shintani Y, Tsutsumi T, Matsuura Y, et al. Subcellular localization of hepatitis C virus structural proteins expressed in transgenic liver. Jpn J Med Sci Biol 1997;50:169–77.
18. Sasaki Y. Does oxidative stress participate in the development of hepatocellular carcinoma? J Gastroenterol 2006;41:1135–48.
19. Moriya K, Nakagawa K, Santa T, Shintani Y, Fujie H, Miyoshi H, et al. Oxidative stress in the absence of inflammation in a mouse model for hepatitis C virus-associated hepatocellular carcinogenesis. Cancer Res 2001;61:4365–70.

20. Moriya K, Todoroki T, Tsutsumi T, Fujie H, Shintani Y, Miyoshi H, et al. Increase in the concentration of carbon 18 monounsaturated fatty acids in the liver with hepatitis C: analysis in transgenic mice and humans. Biophys Biochem Res Commun 2001;281: 1207–12.
21. Okuda M, Li K, Beard MR, Showalter LA, Schole F, Lemon SM, Weinman SA. Mitochondrial injury, oxidative stress, and antioxidant gene expression are induced by hepatitis C virus core protein. Gastroenterology 2002;122:366–75.
22. Tsutsumi T, Suzuki T, Moriya K, Yotsuyanagi H, Shintani Y, Fujie H, et al. Intrahepatic cytokine expression and AP-1 activation in mice transgenic for hepatitis C virus core protein. Virology 2002;304:415–24.
23. Tsutsumi T, Suzuki T, Moriya K, Shintani Y, Fujie H, Miyoshi H, et al. Hepatitis C virus core protein activates ERK and p38 MAPK in cooperation with ethanol in transgenic mice. Hepatology 2003;38:820–8.
24. Miyamoto H, Moriishi K, Moriya K, Murata S, Tanaka K, Suzuki T, et al. Hepatitis C virus core protein induces insulin resistance through a PA28γ-dependent pathway. J Virol 2007;81:1727–35.
25. Shintani Y, Fujie H, Miyoshi H, Tsutsumi T, Kimura S, Moriya K, et al. Hepatitis C virus and diabetes: direct involvement of the virus in the development of insulin resistance. Gastroenterology 2004;126:840–8.
26. Perlemuter G, Sabile A, Letteron P, Vona G, Topilco A, Koike K, et al. Hepatitis C virus core protein inhibits microsomal triglyceride transfer protein activity and very low density lipoprotein secretion: a model of viral-related steatosis. FASEB J 2002; 16:185–94.
27. Moriishi K, Mochizuki R, Moriya K, Miyamoto H, Mori Y, Abe T, et al. Critical role of PA28γ in hepatitis C virus-associated steatogenesis and hepatocarcinogenesis. Proc Natl Acad Sci USA 2007;104:1661–6.
28. Tsutsumi T, Suzuki T, Shimoike T, Moriya K, Yotsuyanagi H, Matsuura Y, et al. Interaction of hepatitis C virus core protein with retinoid X receptor-α modulates its transcriptional activity. Hepatology 2002;35:937–46.
29. Peters JM, Cheung C, Gonzalez FJ. Peroxisome proliferator-activated receptor-alpha and liver cancer: where do we stand? J Mol Med 2005;83:774–85.
30. Tanaka N, Moriya K, Kiyosawa K, Koike K, Aoyama T. Hepatitis C virus core protein induces spontaneous and persistent activation of peroxisome proliferator-activated receptor alpha in transgenic mice: implications for HCV-associated hepatocarcinogenesis. Int J Cancer 2008;122:124–31.
31. Akiyama TE, Sakai S, Lambert G, Nicol CJ, Matsusue K, Pimprale S, et al. Conditional disruption of the peroxisome proliferator-activated receptor gamma gene in mice results in lowered expression of ABCA1, ABCG1, and apoE in macrophages and reduced cholesterol efflux. Mol Cell Biol 2002;22: 2607–19.
32. Tanaka N, Moriya K, Kiyosawa K, Koike K, Gonzalez FJ, Aoyama T. PPAR-α is essential for severe hepatic steatosis and hepatocellular carcinoma induced by HCV core protein. J Clin Invest 2008;118:683–94.
33. Kinzler KW, Vogelstein B. Lessons from hereditary colorectal cancer. Cell 1996;87:159–70.
34. Koike K. Molecular basis of hepatitis C virus-associated hepatocarcinogenesis: lessons from animal model studies. Clin Gastroenterol Hepatol 2005;3:S132–5.

**Research Article** **Chromatography**

Received: 31 July 2008, Revised: 7 August 2008, Accepted: 7 August 2008 Published online in Wiley Interscience: 2008

(www.interscience.wiley.com) DOI 10.1002/bmc.1139

# Limitation of immunoaffinity column for the removal of abundant proteins from plasma in quantitative plasma proteomics

**Tomoko Ichibangase,[a] Kyoji Moriya,[b] Kazuhiko Koike[b] and Kazuhiro Imai[a]***

**ABSTRACT: In plasma proteomics, before a proteome analysis, it is essential to prepare protein samples without high-abundance proteins, including albumin, via specific preparation techniques, such as immunoaffinity capture. However, our preliminary experiments suggested that functional changes with use alter the ability of the immunoaffinity column. Thus, in this study, to evaluate the changes of the removal ability of abundant proteins from plasma by the immunoaffinity column, plasma proteome analysis was performed for the long-term test for the reproducibility of the affinity column using the fluorogenic derivatization–liquid chromatography–tandem mass spectrometry method combined with an IgY column. The specific adsorption for albumin decreased with an increase in the number of the column usage before its expiration date. Moreover, it was demonstrated that hydrophobic high molecular weight compounds in plasma adsorbed onto the column materials surface contributed to the functional changes from specific immunoaffinity adsorption into hydrophobic interaction. These results suggested that, in quantitative plasma proteomics studies, it is important to keep in mind the risk of not only the nonselective loss but also the changes in the adsorption ability of the immunoafinity column. Copyright © 2008 John Wiley & Sons, Ltd.**

**Keywords:** plasma; proteomics; immunoaffinity column; abundant protein; FD-LC-MS/MS method

## Introduction

Blood samples can be taken at a particular point in time with little burden on patients and the constituents of the blood samples could reflect a developing or existing illness because tissue-specific proteins may be released into the brood stream from the damaged or dead cells. Therefore, it is generally recognized in proteomics studies that blood samples represent the greatest potential source of information on the proteins related to human diseases. However, plasma proteome analysis aiming at quantitative protein profiling and biomarker discovery is not easily done. Since several high-abundance proteins, such as albumin, typically constitute greater than 90% of total protein mass, the detection of lower-abundance proteins which presumably are the biologically interesting population is interfered with by the dominant proteins. To address the complexity of these samples, it is essential to prepare samples via specific preparation techniques to remove high-abundance proteins from the samples before the proteome analysis (Linke *et al.*, 2007; Martosella *et al.*, 2005; Qian *et al.*, 2006; Steel *et al.*, 2003). There are a number of approaches for removing proteins based on their biochemical and biophysical features, such as molecular weight, mass, density, hydrophobicity, surface change and isoelectric point. Among these techniques, immunoaffinity capture using antibodies is rapidly becoming the prefractionation method of choice in proteomics analysis. Commercial kits using an avian immunoglobulin yolk (IgY) have recently become available due to its high avidity and lesser cross-reactivity with heterologous human proteins (Huang *et al.*, 2005; Linke *et al.*, 2007; Qian *et al.*, 2006). A number of researchers have already indicated its utility and the improvement of the detection of low-abundance proteins by the elimination of the high-abundance proteins using the IgY affinity column (Gong *et al.*, 2006; Huang *et al.*, 2005; Linke *et al.*, 2007; Liu *et al.*, 2006; Qian *et al.*, 2006).

We have recently developed a highly sensitive and quantitative proteomics method called fluorogenic derivatization–liquid chromatography–tandem mass spectrometry (FD-LC-MS/MS) (Masuda *et al.*, 2004; Toriumi and Imai, 2003). The method consists of separation of the fluorogenic derivatized proteins by high-performance liquid chromatography (HPLC), isolation of the target protein obtained by HPLC, hydrolysis and identification of the target protein by LC-MS/MS with the probability-based protein identification algorithm. This highly selective, sensitive and reproducible method enables the post-translational proteins and isoforms to be distinguished. The method was applied to the extracts of *Caenorhabditis elegans*, mousee liver and breast cancer cell lines, and revealed the proteins related to early-stage Parkinson's

* Correspondence to: K. Imai, Research Institute of Pharmaceutical Sciences, Musashino University, 1-1-20 Shinmachi, Nishitokyo-shi, Tokyo 202-8585, Japan. E-mail: k-imai@musashino-u.ac.jp

[a] Research Institute of Pharmaceutical Sciences, Musashino University, Tokyo, Japan

[b] Department of Internal Medicine, Graduate school of Medicine, University of Tokyo, Tokyo, Japan

**Abbreviations used:** DAABD-Cl, 7-Chloro-*N*-[2-(dimethylamino)ethyl]-2,1,3-benzoxadiazole-4-sulfonamide; FD, fluorogenic derivatization; HCCA, α-cyano-4-hydroxycinnamic acid; TCEP, Tris (2-carboxyethyl) phosphine hydrochloride; TFA, trifluoroacetic acid; TOF, time-of-flight.

Contract/grant sponsor: MEXT HAITEKU (2004–2008), Grant-in-Aid for Young Scientists (Start-up).

Contract/grant sponsor: Mochida Memorial Foundation for Medical and Pharmaceutical Research.

 

disease (Ichibangase *et al.*, 2008), hepatocarcinogenesis (Ichibangase *et al.*, 2007) and tumor progression and metastasis (Imai *et al.*, 2008). During the course of our studies, we applied the FD-LC-MS/MS method to plasma proteomics. To detect plasma biomarkers that are probably masked by the high-abundant proteins, an IgY affinity column was utilized for the removal of the dominant proteins, such as albumin, from plasma before the fluorogenic derivatization (FD) of the plasma proteins. On the preliminary experiments, the quantitative changes of the peaks on the chromatograms obtained from the same samples were observed on every occasion of sample treatment with the affinity column. Since the detectability of the fluorogenic derivatized proteins by the HPLC-fluorescence detector is always constant, the change in the removal ability of the IgY column for the abundant proteins could be monitored during the usage of the column. Although it was reported that there was a risk of loss by inadvertent capture of low-abundance proteins (Bjorhall *et al.*, 2005; Gong *et al.*, 2006; Linke *et al.*, 2007; Plavina *et al.*, 2007; Yocum *et al.*, 2005), there are no reports of long-term tests for the reproducibility of the affinity column in quantitative proteome analysis.

In this study, to evaluate the removal ability of abundant proteins from plasma by the affinity column, we performed proteome analysis of plasma sample and protein standards by FD-LC-MS/MS combined with the IgY technique and investigated the cause of the quantitative changes of the chromatograms mentioned above.

## Experimental

### Materials and Methods

**Reagents.** 7-Chloro-*N*-[2-(dimethylamino)ethyl]-2,1,3-benzoxadiazole-4-sulfonamide (DAABD-Cl) and 6.0 M guanidine hydrochloride (pH 8.7 buffer solution) were purchased from Tokyo Chemical Industry (Tokyo, Japan). Ethylenediamine-*N*,*N*,*N*′,*N*′-tetraacetic acid sodium salt ($Na_2EDTA$) and 3-[(3-Cholamidopropyl) dimethyammonio]-1-propanesulfonate (CHAPS) were from Dojindo Laboratories (Kumamoto, Japan). Tris (2-carboxyethyl) phosphine hydrochloride (TCEP) was obtained from Sigma-Aldrich (St Louis, MO, USA). Acetonitrile and trifluoroacetic acid (TFA) for the HPLC-fluorescence detection were HPLC grade and were obtained from Wako Pure Chemical Industries (Osaka, Japan). All other reagents used were of analytical grade.

### Affinity Columns

The prepacked IgY-R7 Spin Column and Seppro®-IgY12 were obtained from Beckman Coluter (Fullerton, CA, USA) and GenWay Bioteck (San Diago, CA, USA), respectively. The IgY-R7 Spin Column (1.2 mL spin column) removes seven high-abundance proteins in rodent plasma (albumin, IgG, $\alpha$2-antitrypsin, IgM, transferring, haptoglobin and fibrinogen) and utilizes centrifugation as the force for affinity separation. The column is said to be reusable 100 times under proper conditions. The Seppro®-IgY12 column is optimized for human plasma and removes 12 high-abundance proteins (IgA, $\alpha$1-acid glycoprotein, $\alpha$2-macroglobin, apolipoproteins A-I and apolipoproteins A-II besides the above seven proteins). This column is used with the high-throughput automated proteomic sample processing instrument (Magtration System SA-1; Precision System Science, Chiba, Japan) and is said to be able to be used 30 times. Both companies are corporate partners for the exclusive marketing of the IgY microbeads technology, and both column materials are the same except for recognized animal species to the IgY.

### Plasma Samples

For the IgY-R7 Spin Column, plasma sample were obtained from C57BL/6N male mice (10 and 19 months; Clea Japan, Tokyo, Japan) by centrifugation at 5510 rpm for 10 min at 4°C, and frozen at −80°C until use. On the other hand, the human control plasma sample purchased from Sigma-Aldrich was used for the Seppro®-IgY12 column. The control plasma sample was passed through a 0.45 μm filter before use.

### Treatment of Mouse Plasma with the IgY-R7 Spin Column

Mouse plasma treated with the spin column was carried out according to the manufacturer-instructed column usage and loading capacity [10 μL plasma diluted with dilution/washing buffer: 10 mM Tris–HCl, 150 mM NaCl, pH 7.4 (TBS)]. Three buffers (dilution/washing buffer; stripping buffer: 100 mM glycine, pH 2.5; neutralization buffer: 100 mM Tris–HCl, pH 8.0) were used under the separation scheme that consisted of sample loading–washing–eluting–neutralization followed by a re-equilibration scheme for a total cycle time of 40 min. To increase the recovery of the non-specific proteins, the resulting flow-though fraction and the washing fractions were collected and concentrated to 10 μL with 3.0 kDa molecular weight cutoff device according to the manufacturer's instructions (Microcon YM-3; Millipore, Billerica, MA, USA).

### Treatment of Protein Standards and Control Human Plasma Sample with the Seppro®-IgY12 Column

The molecular weight standards, consisting of phosphorylase B, serum albumin, ovalbumin, carbonic anhydrase, trypsin inhibitor and lysozyme for electrophoresis (Table 1; 12 mg/mL protein amount; low range; Bio-Rad, Herccules, CA, USA), were employed in sample processing without dilution to evaluate the recovery of non-specific proteins from the column. The injected amount of the protein standards was 2.4 mg protein per injection to the affinity column. Since, in the instructions, 15 μL of plasma (generally corresponding to 70–80 mg proteins/mL) was diluted to 500 μL and loaded to the affinity column, the injected amount of the standards was compatible. According to the manufacturer's instructions, the protein standards were set in the sample holding and then the flow-though fraction was obtained.

The control human plasma sample was also treated according to the manual. Briefly, 15 μL of plasma sample was diluted with the dilution/washing buffer to 500 μL, and the sample was set in the sample holding, as in the case of the protein standards. The resulting flow-though fraction of the plasma was concentrated

**Table 1.** Protein standards and the number of labeled region with DAABD-Cl

| Protein | Source | MW (kDa) | No. of rabeled region |
|---|---|---|---|
| Phosphorylase B | Rabbit muscle | 97.4 | 10 |
| Serum albumin | Bovine | 66.2 | 35 |
| Ovalbumin | Hen egg white | 45 | 5 |
| Carbonic anhydrase | Bovine | 31 | 2 |
| Trypsin inhibitor | Soybean | 21.5 | 5 |
| Lysozyme | Hen egg white | 14.4 | 6 |

  

to 15 μL with a Microcon YM-3 device. A series cycle including the sample loading–washing–eluting–neutralization finished in 65 min.

### FD-LC-MS/MS Conditions

Each FD condition was optimized for the protein standards and for plasma samples in order to obtain the highest peak on the chromatograms. For the protein standards, a 2.5 μL aliquot of the flow-though fraction was mixed with 30 μL of a mixture of 0.83 mM TCEP, 3.3 mM $Na_2EDTA$ and 16.6 mM CHAPS in the pH 8.7 buffer solution, 12.5 μL of the buffer solution and 5.0 μL of 8.0 mM DAABD-Cl in acetonitrile. The mixture was reacted at 50°C for 5.0 min, and the reaction was stopped with 1.5 μL of 20% TFA. A 20 μL aliquot of the above reaction mixture was injected to the HPLC system (Hitachi L-2000 series; Hitachi Instruments, Tokyo, Japan) using a column of Intrada WP-RP (30 nm pore size, 250 × 4.6 mm i.d., Imtakt Co, Kyoto, Japan) at 60°C with a flow rate of 0.55 mL/min. The eluent (A) and eluent (B) were water–acetonitrile–TFA (90:10:0.15, v/v/v) and water–acetonitrile–TFA (30:70:0.05, v/v/v), respectively. The gradient condition was established from 5 to 100% eluent (B) over a period of 60 min. For mouse and control plasma samples, a 6.0 μL aliquot of the flow-though fraction was mixed with 30 μL of the above mixture of TCEP, $Na_2EDTA$ and CHAPS, 10 μL of the buffer solution and 4.0 μL of 825 mM DAABD-Cl in dioxane. After the FD reaction (50°C for 5.0 min), the reaction was stopped with 2.0 μL of 20% TFA. An aliquot (10 μL) of the reaction mixture was injected, and the longer column (Intrada WP-RP 30 nm pore size, 500 × 4.6 mm i.d., Imtakt Co) together with a precolumn (Intrada WP-RP 30 nm pore size, 5.0 × 2.0 mm i.d., Imtakt Co) at 60°C was adopted with a flow rate of 0.55 mL/min on the HPLC system. The mobile phases consisted of water–acetonitrile–TFA (A) 90:10:0.15 and (B) 30:70:0.05. Mobile phase (C) was the same as (A), except with 0.05% TFA. The gradient condition is described in Fig. 1. Fluorescence detection was carried out at 395 and 505 nm for the excitation and emission wavelengths, respectively. The peak height of each protein peak obtained from the HPLC chromatograms was calculated by HITACHI EZChrom Elite™ Chromatography Data System (Hitachi Instruments) and the identification of the standard proteins was accomplished according to the previous report (Ichibangase *et al.*, 2007).

### Scanning Electron Microscopy and Matrix-assisted Laser Desorption/Ionization MS Analysis

Scanning electron microscopy (SEM) and matrix-assisted laser desorption/ionization (MALDI) MS analyses were conducted in Jeol Datum (Tokyo, Japan) and Bruker Daltonics Japan (Kanagawa, Japan), respectively.

For SEM analysis, the column materials were diluted with phosphate buffer (300 mOsm) and fixed with fixative (2.5% glutaraldehyde in PBS, pH 7.0) for 10 min. The fixed sample was captured on the filter (SEM-Pore: 0.6 μm i.d.; 10 μm) and washed with the buffer. After the osmium-fix (2% $OsO_4$) and a brief rinse with the fixative solutions, specimens were dehydrated in a series of graded ethanol (30–100%). The immersed specimens in ethanol were replaced with isoamyl phenylacetate and subjected to critical point drying. The dried samples were coated with osmium using a plasma coater (OPC80N, Jeol). Images were acquired using a Jeol JSM-7401F in normal SEM mode. For the low power microscope images for the whole picture of a material, a lower electron image (LEI) was applied.

For MALDI MS analysis, the column materials were washed and spotted on a plate. α-Cyano-4-hydroxycinnamic acid (HCCA) was used as matrix. MALDI mass spectra were acquired with time-of-flight (TOF) MS (autoflex III, Bruker Daltonics) in positive linear mode.

## Results and Discussion

### Quantitative Functional Changes of the IgY-R7 Spin Column after a Number of Treatments with Mouse Plasma

For the detection of low-abundance proteins in mouse plasma, the removal of high-abundance proteins from mouse plasma with the affinity column was performed prior to the FD-LC-MS/MS proteome analysis. Typical chromatograms are shown in Fig. 1(A), obtained from the same mouse plasma sample treated with 80 and 86 cycles of the same spin column, respectively. All peak heights obtained from the 86 cycles of the spin column were clearly higher compared with those obtained from the 80 cycles. Although a difference between column lots might exist, there were also significant differences in the removability of the affinity column between the second (column lot no. 2) and the 44th cycles (column lot no. 1) of the treated spin column [Fig. 1(B)]. The relative standard deviation (RSD) of the protein peaks was calculated between-day ($n = 3$) using samples provided by the same treatment number of the column. The RSD values were less than 21.6%, obtained from the peak in Fig. 1(A), suggesting that the detectability of the fluorogenic derivatized proteins by HPLC is constant. Therefore, it was considered that the quantitative changes of the peaks on the chromatograms might result from the changes in the affinity column by the sample treatment.

### Evaluation of Seppro®-IgY12 Column for the Adsorption of Protein Standards using an Automatic Instrument

To eliminate a manual usage error from the sample processing, a high-throughput automated instrument, SA-1, for the removal of high-abundance proteins from human plasma samples with a Seppro®-IgY12 column was investigated. For the evaluation of the exact adsorption ratio of specific and non-specific proteins to the affinity column, the affinity column was periodically treated with protein standards after treatment with a control human plasma sample some dozen times. Since the other investigator has reported the non-specific adsorption of the protein by concentration methods such as a centrifugal filter to be about 15% (Linke *et al.*, 2007), the flow-through fraction of the injected protein standards from the affinity column was subjected directly to the FD-LC-MS/MS analysis without a protein concentration step in this study.

At first, to eliminate the non-specific adsorption to the affinity column, the protein standards mixture was divided into two parts and one was subjected into the untreated affinity column, and the flow-though fraction was derivatized with the fluorogenic reagent, DAABD-Cl, and separated by the HPLC system (4.8 μg protein/HPLC injection). Another part of the protein standards mixture was diluted and derivatized with DAABD-Cl, and injected onto the HPLC system (4.8 μg protein/HPLC injection). The obtained chromatograms are depicted in Fig. 2. Each protein peak was collected, digested in peptide mixtures, and identified by applying the peptides to HPLC-MS/MS with a

  

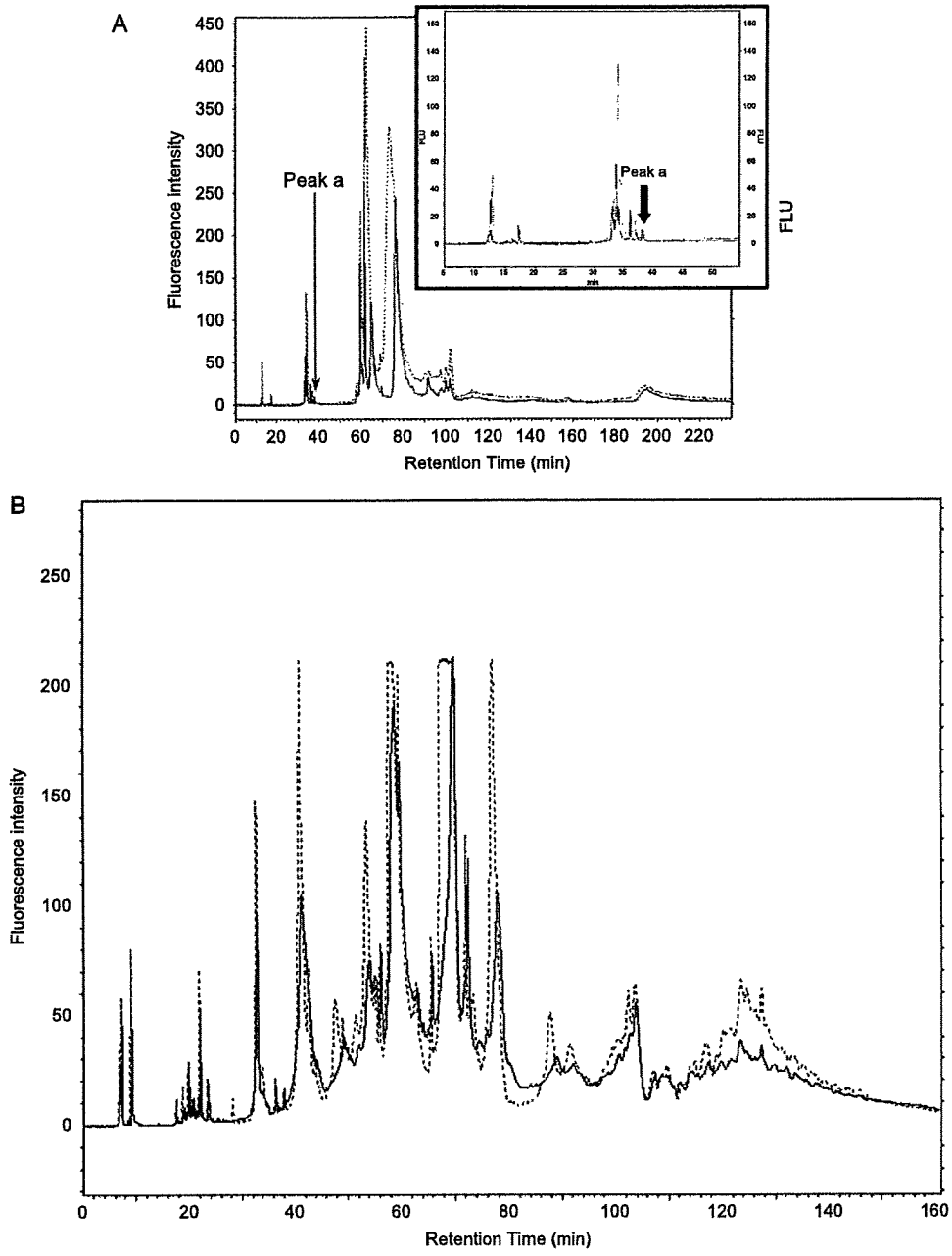


**Figure 1.** Chromatograms of mouse plasma samples treated with IgY-R7 Spin Columns. (A) The mouse plasma (19 months, C57BL/6N) treated 80 times (solid line) and 86 times (dotted line) in the same spin column. The gradient conditions were as follows: time (min), 0 → 10 → 20 → 44 → 48 → 68 → 80 → 90 → 108 → 120 → 130 → 160 → 180 → 230; B (%): 5 → 5 → 30 → 30 → 35 → 38 → 39.2 → 39.2 → 42 → 43 → 44 → 45 → 47 → 58; C (%): 0 → 0 → 0 → 0 → 0 → 0 → 0 → 60.8 → 58 → 57 → 56 → 55 → 53 → 42. (B) The mouse plasma samples (10 months, C57BL/6N) were treated with the second cycle (column lot no. 2; solid line) and the 44th cycle (column lot no. 1; dotted line) of each spin column. The gradient conditions were as follows: time (min), 0 → 5 → 10 → 22 → 24 → 34 → 54 → 60 → 60.1 → 80 → 130 → 140 → 150 → 160 → 170; B(%): 5 → 5 → 30 → 30 → 35 → 38 → 42 → 43 → 43 → 47 → 58 → 60 → 60 → 75 → 78; C(%): 0 → 0 → 0 → 0 → 0 → 0 → 0 → 0 → 57 → 53 → 42 → 40 → 40 → 25 → 22.

database-searching algorism. Table 2 shows the adsorption ratio of the proteins to the untreated column and the identified protein names. The protein names of peak 1 and 2 could not be identified since these peaks were peptides coexisting in the protein standards. Also, carbonic anhydrase and ovalbumin could not be detected. Since carbonic anhydrase has only two cycteine residue for labeling with DAABD-Cl, its detection might be difficult. The reason for the undetected ovalbumin was not clear. Since this study was aimed at investigating the changes in the adsorption of the specific and non-specific proteins using the column, this issue was not examined further. Consequently, although the affinity column was able to efficiently remove bovine serum

  

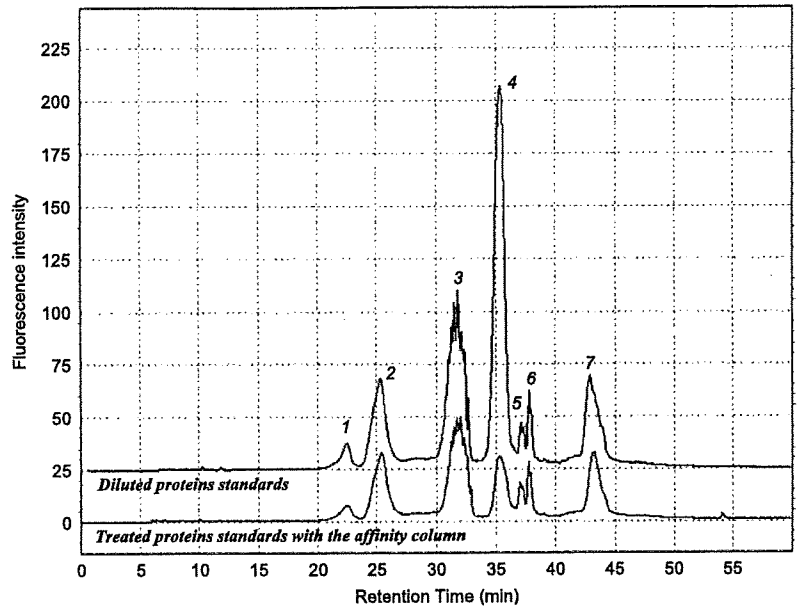


**Figure 2.** Chromatograms of the protein standards which were treated with Seppro®-IgY12 column and diluted to the same protein amount (4.8 μg/HPLC injection) as the amount for the column treatment. The peak numbers correspond to Table 2.

**Table 2.** Adsorption ratio to the untreated Seppro®-IgY12 column and protein names obtained by FD-LC-MS/MS method

| Peak no. | Adsorption ratio to the untreated Seppro®-IgY12 | Protein name |
|---|---|---|
| 1 | 38.5% | Peptide |
| 2 | 30.6% | Peptide |
| [a]3 | 45.9% | Lysozyme |
| 4 | 83.9% | Bovine serum albumin (BSA) |
| [b]5 | 18.3% | Trypsin inhibitor |
| 6 | 28.5% | Trypsin inhibitor |
| 7 | 30.4% | Phosphorylase B |

[a]3, [b]5: Most highest peak

albumin (BSA; 83.9%) as compared with the other proteins in the standards, non-specific binding to the column materials or to carrier proteins such as albumin itself was observed in the 18.3–45.9% range and could result in the loss of presumed biomarkers.

Next, the time series changes of the specific and non-specific adsorption of proteins to the column were investigated. The protein standards mixture was treated with the column periodically after 10 and 20 cycles of treatment of the control plasma sample. The relation of the changes of the protein standards adsorption to the number of uses of the affinity column is shown in Fig. 3(A). The specific adsorption of BSA decreased with an increase in the number of times the column was used. However, the non-specific adsorption for lysozyme, trypsin inhibitor and phosphorylase B reached a maximum at 11 cycles and decreased at 21 cycles. Since the affinity column was optimized for human plasma, the absorption of BSA for the column might be weaker than for plasma albumin. However, the adsorption of albumin in control plasma also decreased with an increase in the number of times the column was used (data not shown). Moreover, since the slopes of decrease differed among the protein standards, the correlation of each adsorption with molecular weight of each protein was calculated [Fig. 3(B)]. The open dots show the value of BSA in Fig. 3(B). The correlation coefficient value was the closest to 1.00 ($R^2 = 0.813$) for 21 cycles [Fig. 3(B-3)], demonstrating that the adsorption ability of the column does not depend any longer on the affinity of the antibody but on the hydrophobicity of the protein. In contrast, the correlation of the values obtained from the first cycle [Fig. 3(B-1); $R^2 = 0.077$] was not fairly observed between the adsorption ability and the hydrophobicity, and the value for BSA was apart from those for other proteins. Therefore, BSA was specifically removed as compared with the other protein standards by the immunoaffinity adsorption. Also, as shown in Fig. 3(B-2), the result obtained from 11 cycles ($R^2 = 0.012$) demonstrated that all proteins bound to the surface of the affinity column materials equally. Therefore, the present data demonstrates that the quantitative changes of the adsorption for the affinity column appear before the limited use of the column (30 times in the manufacturer's instructions).

### Understanding the State of the Plasma-treated Column Materials

To understand the state of the column materials of the Seppro®-IgY12 column, the untreated and 11- and 21-times-treated column materials were subjected to electron microscopy and MALDI-TOF-MS analysis.

As shown in Fig. 4, the SEM images show an obvious difference between the untreated and treated materials. The attachment of the unknown bio-molecules to the materials surface appeared and increased with an increase in the number of treatments.

Next, in order to characterize the attached compounds, the same materials were subjected to MALDI-TOF-MS analysis. Since

  